An-Najah National University

Faculty of Graduate Studies

INVESTIGATION OF ELECTRICAL, OPTICAL AND MORPHOLOGICAL PROPERTIES OF SILVER NANOPARTICLES (Ag NPs) SYNTHESIZED BY MICROWAVE-ASSISTED (MW) SYNTHESIS METHOD

By

Shahd S. F. Habbash

Supervisors

Dr. Muna Hajj Yahya

Dr. Maen Ishtaiwi

This Thesis is submitted in Partial Fulfillment of the Requirements for the Degree of Master of Physics, Faculty of Graduate Studies, An-Najah National University, Nablus – Palestine

2025

INVESTIGATION OF ELECTRICAL, OPTICAL AND MORPHOLOGICAL PROPERTIES OF SILVER NANOPARTICLES (Ag NPs) SYNTHESIZED BY MICROWAVE-ASSISTED (MW) SYNTHESIS METHOD

By

Shahd S. F. Habbash

This Thesis was Defended Successfully on 29/1/2025 and approved by:

Dr. Muna Hajj Yahya	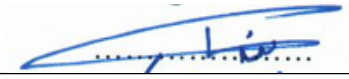
Supervisor	Signature
Dr. Maen Ishtaiwi	
Co-Supervisor	Signature
Dr. Rabab Jarrar	
External Examiner	Signature
Prof. Sami AL Jaber	
Internal Examiner	Signature

Dedication

I dedicate my thesis to my great loving mother and to my father's generous heart, who never stopped believing in me. To my lovely husband, who has been my most profound inspiration, Ahmad. To my beautiful son, the light of my life, Mohammad. To my sister and brothers, the shining stars in my days. To my second family that God has blessed me with, my husband's family. To all supportive family and friends. To my supervisors, Dr. Muna Hajj Yahya and Dr. Maen Ishtaiwi who provided me with sufficient encouragement and knowledge to complete my study. To all my distinguished teachers.

To the challenges that made me stronger. The sleepless nights, doubts and fears. To the heroes who walk among us. To every moment that brought me to this point. To the countless cups of coffee. For all of that I am thankful.

Shahd S. Habbash

Acknowledgments

First of all, I acknowledge my thanks to Allah, the Ever-Thankful; the Ever-Magnificent for his blessing to me and for the strength he give me each day. I can't do it without his guidance. I would like to express my deep gratitude to my thesis supervisors, Dr. Muna Hajj Yahya and Dr. Maen Ishtaiwi for their exceptional guidance, valuable advice and constant support through this work. And many thanks to Dr. Shadi Sawalha for his especial help during the study. I am also grateful to the laboratories of physics, chemical engineering and pharmacy for access to equipment and essential resources that made my research possible. Last and not least, I would like to say thanks to my family for their support during the intense moments of thesis writing.

Shahd S. Habbash

Declaration

I, the undersigned, declare that I submitted the thesis entitled:

INVESTIGATION OF ELECTRICAL, OPTICAL AND MORPHOLOGICAL PROPERTIES OF SILVER NANOPARTICLES (Ag NPs) SYNTHESIZED BY MICROWAVE-ASSISTED (MW) SYNTHESIS METHOD

I declare that the work provided in this thesis, unless otherwise referenced, is the researcher's own work, and has not been submitted elsewhere for any other degree or qualification.

Student's Name: شهد سعدالله فايق هباش

Signature: شهد هباش

Date: 29/1/2025

List of Contents

List of Tables

List of Figures

List of Appendices

INVESTIGATION OF ELECTRICAL, OPTICAL AND MORPHOLOGICAL PROPERTIES OF SILVER NANOPARTICLES (AG NPS) SYNTHESIZED BY MICROWAVE-ASSISTED (MW) SYNTHESIS METHOD

By

Shahd S. F. Habbash

Supervisors

Dr. Muna Hajj Yahya

Dr. Maen Ishtaiwi

Abstract

Nanoparticles (NPs) are very small-sized particles with a diameter ranging between 1 to 100 nm. Metallic nanoparticles take a huge place in recent researches because of its importance in different fields; electrical, optical, industrial and more. Among the known metals, silver (Ag) is the most especial one due to its physical and chemical properties. Several methods were used to prepare silver nanoparticles. The microwave-assisted synthesis method (MW) is the easiest way in which the Ag NPs can be synthesized in a very short time (some seconds), with high yield and controlled synthesis conditions.

In this study, the Ag NPs were successfully prepared using the MW method. In the preparation process we used the precursor Silver Nitrate ($AgNO_3$), with Ethylene Glycol as a reducing agent and polyvinylpyrrolid (PVP) as a stabilizing agent. The synthesis conditions were controlled during the preparation method. These conditions are the power of the microwave (Medium-Low, ML, Medium, M, Medium-High, MH, and High, H), the microwave heating time (30s and 90s) and the ratio between the precursor to stabilizing agent, $AgNO_3$: PVP $(1:1/2, 1:1, 1:2, 1:3)$.

The prepared samples were characterized using the ultra-violet visible absorption spectroscope (UV-vis). It is clear that both times can be used successfully to prepare Ag NPs, this is obtained from the peak of surface-plasmon resonance band (SPR) which exist in the correct region $(400 - 450)$ nm.

The atomic force microscope (AFM) was used to study the morphological properties of the prepared samples (size and shape). All samples have a spherical shape of the Ag NPs with different sizes. An enhancement of the Ag NPs size occurs by either increasing the MW power, increasing the MW heating time, or decreasing the PVP ratio.

The electrical properties of the same samples were studied using the vector network analyzer (VNA). The 30s samples are not stable, while the 90s samples give stable measurements, and repeating measurement process after a long time (up to 7 months) gives approximately the same results for these 90s samples.

Keywords: Nanoparticles; Silver Nanoparticles; Microwave-assisted synthesis method; Ultraviolet-Visible Absorption Spectroscopy; Atomic Force Microscopy; Vector Network Analyzer.

Chapter One

Introduction and Theoretical Background

Nanoscience has become a great field of physics. The use of nanomaterials has spread dramatically in recent years. Nanoparticles (NPs) are defined as very small-sized particles with a diameter ranging between 1 and 100 nanometer (nm) (1). They can be categorized according to the type of material into semiconductor, polymeric and metallic nanoparticles (2). Nano-scale structures can be formed from several metal and metalloid elements like gold (Au), Silver (Ag) and Iron-based magnetic nanoparticles (3). Among the metals, silver nanoparticles (Ag NPs) show potential applications in various fields such as the environment, bio-medicinal, catalysis, optics and electronics (4). Several methods have been used to prepare Ag NPs. The abundance of these methods can be divided into two basic synthesis ways, namely top-down and bottom-up (5). Microwave (MW) assisted synthesis is one of these methods, it is based on the interaction that occurs between the polar solvent molecules and/or ions inside the solution with electromagnetic_waves. This direct interaction results in homogeneous heating and high heating rates with high-energy efficiency and shorter preparation time (6). Through the last few years, the synthesis of NPs has been growing quickly for different applications, such as; electronics, chemistry, biology…etc (7).

The aim of this study is to prepare Ag NPs by the microwave-assisted method. Different parameters will be controlled during the work, these parameters include the MW power, the MW heating time and the stabilizing agent ratio. A detailed study of the electrical, optical and morphological properties of the prepared solutions which contains Ag NPs will be done. According to the results that we will obtain, suitable applications will be considered.

1.1 Introduction to Nanoparticles

Nanotechnology defined as the achievement of obtaining particles in a small size ranging between $1-100$ nm. Due to the decrease in the length of the material to become in nanometer, their properties will change. This is due to surface-area effects which becomes more important, and the quantum effects occur (8).

The surface-area effect of the nanoparticles comes from the larger number of atoms which found on the surface compared to the same type of material in the bulk form. The more atoms in the surface will enhance the chemical reactions of this material, and hence improve their properties (9).

The physical properties of any material can be described by the average of the quantum effects acting on each atom. In the nanoparticles, the size of particle is very small and sharp. This makes it possible for the quantum effect which acts on one small atom to decide the properties of these NPs. In the bulk material, the electron can move freely between the atoms. While in the size of nanometer for particles, the electron wave function is comparable to the size of the particles and feels the boundaries of the atom. This causes a confinement of the energy levels that the electron can exist in (10).

Materials prepared in nanoscale can have different dimensions: The zero dimension, which means all the 3D are in nanoscale and no dimensions outside (in this case nanoparticles were obtained), in the 1 dimension, there is one dimension outside the nanoscale (like nanotubes and nanofibers),the 2 dimensions have one dimension in the nanoscale (nanolayers or nanofilms), and the 3 dimensions have none of the dimensions in the nanoscale (nanocomposites and nanostructured) (11).

1.2 Silver Nanoparticles (Ag NPs)

Silver (Ag) is a white lustrous metal which located in period 5 and group 11 (Ih) in the periodic table. Special properties of this element make it a valuable one. It has the highest known electrical and thermal conductivity of all metals. Its electrical conductivity is $6.3 \times 10^7 \mathrm{s/m}$ at$20^{\circ}\mathrm{C}$ (12). Moreover it has a high resistance to atmospheric oxidation, malleability and ductility. These good properties make it widely used in fabrication processes and as a coating for electronic conductor (13).

In the last years, there is an increase in the synthesis and uses of Nano-materials in several applications. The controlled particle size, high surface area and particle morphology (size and shape) gives high reactivity to Silver nanoparticles. Ag metal is expected to be a good choice to use as a metallic nanoparticles. This is because of the chemical stability and catalytic effect of it which has benefits for antibacterial, anticancer and antifungal activities. Moreover, the Ag is special element because of their nontoxicity towards the human (14).

1.3 Methods of preparing Nanoparticles

Several methods have been used to prepare Ag NPs. The abundance of these methods can be divided into two basic synthesis ways, namely top-down and bottom-up.

1.3.1 Top-down Approach

Top-down methods involve the creating of nanoscale materials starting from bulk material by reducing their size through "cutting" to reach the required value (15). Some examples of this approach were summarized in table.1. Each method has advantages, disadvantages and applications (16).

Table 1

Examples of top-down synthesis approach with advantages, disadvantages and applications

Method	Advantages	Disadvantages	Applications
Ball milling	• Large scale production of high purity nanoparticles. • Improved properties to the component.	• High energy required. • Long period of milling time. • Very sensitive microstructure.	• Mechanical alloying
Laser ablation	• Relatively simple and effective technique. • Controlled laser parameter.	• Prolong time laser ablation. • Reduction in ablation rate.	• Preparation of Al_2O_3 NPs coating. • Preparation of silicon NPs.
Ion sputtering	• Economical method. • Controlled of different parameters due to slow deposition of heavier atoms.	• The nature sputtering gas can produce effect on surface morphology and composition.	• Deposition of large molecules.
Mechanochemical synthesis	• Simple and efficient method of nanoparticle preparation.	• The formed microstructures are sensitive to grinding condition.	• Synthesis of ferric oxide NPs. • Nanocrystalline particle synthesis.

1.3.2 bottom-up Approach

Bottom-up methods use the atomic, molecular, or ionic components to obtain the more complex nanoscaled materials (15). Some methods of this approach were summarized in table.2 (16).

Table 2

Examples of Bottom-up synthesis approach with advantages, disadvantages and applications

Method	Advantages	Disadvantages	Applications
Physical vapor deposition method.	• Simple method for the formation of thin metal films.	• Expensive method. • Generates low volume of material.	• Efficient thin-film solar cells.
Hydrothermal method.	• Desired size and shape NPs. • Well-crystallized powder can be formed.	• Processes are difficult to control. • Limitation of reliability and reproducibility.	• Preparation of powders (as NPs or single crystal.
Microwave assisted preparation method.	• Highly effective. • Simple, rapid volumetric heating. • Homogenous heating.	• Shorter crystallization time.	• Materials science. • plant-based extracts to prepare various metal NPs.
Chemical reduction method	• Simplest method used for preparation of metal nanoparticles.	• Several limitations associated with reducing agents such as toxicity, expensive, poor reducing ability, high costs, and impurities.	• Preparation of copper nanoparticle using potassium borohydrate as a reducing agent.

In this study, Microwave-assisted synthesis method was used. It is an easy, low cost and efficient method to produce Ag NPs in a solution form. More details about this method will be discussed in the next tittle.

1.4 MW-Assisted Synthesis Method

Microwave-assisted synthesis is a type of heating ways which depend on the MW radiation to accelerate chemical reactions and it has been largely used in material synthesis (17).

The working principle of this method based onto aligning dipoles of the sample in an external field under the excitation done by microwave electromagnetic radiations (17). The MW heating method converts the energy of the radiated waves into heat by two major mechanisms; dipolar polarization and ionic conduction. In the first process, when the sample affected by the irradiated microwave frequencies, the molecular dipoles in the sample try to align in the same direction with the applied electric field. An oscillation of this electric field makes the dipoles follow the alternating electric filed. This make a loss of energy as a heat from the friction of sample molecules and dielectric loss. While in the ionic conduction process, the ions (dissolved charged particles) oscillate back and forth when it is affected by an applied electric filed. This oscillations make collisions between neighbor ions, which as a result generate heat. The ability of a given material to convert electromagnetic energy (the microwave energy in our case) into heat can be explained by the concept of loss tangent ($tan\delta$). So, the loss tangent measures the amount of heat generated for a certain degree of rotation (or polarization) (18).

Microwave method has many advantages over the conventional heating processes, this make it widely used in the synthesis of nanomaterials. These benefits can be listed as:

- Rate enhancement: Due to the reduction in activation energy, reaction time is dramatically decreased from hours to minutes or even seconds. So MW method considered to be a fast one compared to other methods of preparation (19).

- High product yield: This happens because of the reduction in the reaction time which will also reduce the side effects like environmental conditions. As a result an increase in the product yield will happen (19).

- Expanded reaction conditions: In the MW method, reaction conditions can be easily controlled unlike conventional methods. This make it easy to make optimization of the parameters to obtain the best conditions (19).

- Ease of synthesis: the MW method is an easy way to produce nanoparticles. The reaction needs a precursor, a reducing agent and a stabilizing agent with some steps of production. And there is a flexibility of choosing them which make it an easy way.

1.5 Properties of Nano-materials

The optimization of Ag NPs will be done by studying their electrical, optical and morphological properties.

1.5.1 Electrical Properties

These properties include real ($\acute{\varepsilon}$) and imaginary ($\acute{\acute{\varepsilon}}$) parts of permittivity, loss tangent, electrical conductivity (σ), Impedance matching ratio ($Z/Z0$), penetration depth (or called skin depth, δ_s), attenuation constant (α), reflection coefficient (R), shielding effectiveness (SE) and scattering parameters (S-parameters).

- **Real and Imaginary Parts of Permittivity**

Permittivity can be defined as a constant of proportionality which make a relation between the electric field in a given material and the electric displacement of that material. It indicates the tendency of electric charge to be polarized in the presence of external electric field. The larger value of polarization means higher permittivity (20).

Permittivity is a measure of the material's ability to influence or modify the electric field of an electromagnetic wave, and it is a dimensionless quantity (21). It is a complex quantity ($\varepsilon_r, \varepsilon_r = \varepsilon' - j\varepsilon''$), where $\acute{\varepsilon}$ represents its ability to store electromagnetic energy (it is also called the dielectric constant), and $\acute{\acute{\varepsilon}}$ represents its ability to attenuate electromagnetic energy (22).

- **Loss tangent**

Loss tangent is defined as the ratio between the energy lost inside the material to the energy stores inside it, when a periodic external electric field exert on it. It is a frequency dependent parameter which shows the efficiency of the material to conserve the energy (23).

The electric loss tangent of a material gives the ability of that material to attenuate the electromagnetic wave when passing through it. Increasing the value of $tan\delta$ of the material meaning that a higher attenuation as the wave travels through the material will occur (21).

- **Electrical conductivity**

Electrical conductivity is the ability of the material to carry current. Its unit is s/m in the SI units. The value of the electrical conductivity for nanomaterials is lower than the bulk materials, this happens because a decrease in the size of the material to become some nanometers leads to an increase in the energy band gap. Which results in lowering the electrical conductivity of the material (24).

- **Impedance matching**

Impedance (Z) is a combination of resistance and reactance. It is essentially anything and everything that obstructs the flow of electrons within an electrical circuit.

Impedance matching is the process where the input impedance and the output impedance of a given electrical load are designed to reduce signal reflection and maximize the power transferred to the electric load (25).

The enhancement of the impedance matching of the material make it suitable for the practical design which improve the microwave absorption performance (26).

- **Penetration depth (skin depth)**

Penetration depth or called skin depth, it is the depth where the intensity is reduced to $1/e$ (about 37%) of the original intensity at the surface (27). It depends of the electrical properties of the material. An increase in the loss factor (denotes by the complex part of permittivity) makes faster microwave energy absorption. It is shown that the incident power density decreases exponentially form the surface to the core region (28).

- **Attenuation constant**

It means how the electromagnetic wave attenuate inside a material. An increase in the attenuation constant cause a high absorption of the wave. The attenuation constant is the reciprocal of the penetration depth.

- **Reflection Coefficient**

It is a measure of the intensity of reflected electromagnetic wave to the intensity of incident wave. High value of R means the material will highly shield the electromagnetic wave incident on it.

The reflection of the electromagnetic waves happens when there is a difference of the impedance between two boundaries. This difference called the impedance mismatch. The larger the impedance mismatch, the larger the value of energy which will be reflected at this interface between the two sides or boundaries (29).

- **Shielding Effectiveness**

Shielding effectiveness (SE) shows the ability of a material to attenuate electromagnetic field. Increasing the value of SE will increase the electromagnetic isolation (30). It can also be defined as the ratio between the magnitudes of the incident and transmitted electric field. The shielding effectiveness value affected by different parameters: the frequency of the incident electromagnetic energy, the shield material parameters (permittivity and conductivity values), the shield thickness, and the type of the electromagnetic field source (electric field, magnetic field or plane wave) (31).

- **Scattering Parameters**

Scattering parameters or called simply S-parameters, are numerical values which describe the electrical behavior of a linear, time-invariant, multi-port network. These parameters determine the relationship between the incident and reflected waves at each network port. So, S-parameters define the transformation of energy between the ports in the given system. These S-parameters are frequency dependent (32). If we have a system of two ports, a_1 and a_2 means the incident waves on port 1 and 2, b_1 and b_2 are the reflected waves at port 1 and 2, respectively, these incident and reflected waves can be related mathematically by the S-matrix as follow:

$$\begin{pmatrix} b_1 \\ b_2 \end{pmatrix} = \begin{pmatrix} S_{11} & S_{12} \\ S_{21} & S_{22} \end{pmatrix} \begin{pmatrix} a_1 \\ a_2 \end{pmatrix} \tag{1.1}$$

Where the diagonal elements of the S-matrix represent the reflection coefficients from the two ports. And the off-diagonal elements represent the transmission coefficients from one port to the other.

1.5.2 Optical Properties

- **Absorbance and Maximum absorption wavelength**

Absorbance (A) is a measure of the quantity of light absorbed by a material (33). λ_{max} is defined as the wavelength that corresponds to the peak of absorbance . It can be used to find the energy of the conduction band (E_c) by the Einstein's photon energy equation:

$$E_c = \frac{hc}{\lambda_{max}} \tag{1.2}$$

Where h is Plank's constant and c is the speed of light.

There is a proof that the optical absorption of metallic nanoparticles can be studied in quantum mechanics due to intra-band excitations of the conduction electrons by photon. In metallic nanoparticles, the conduction electrons are not entirely free as in the bulk material, but some are held by the individual atoms and others are free to move between atoms. The free moving electrons form metallic bonds which cement the metal nanoparticles. At the maximum absorbance wavelength, the conduction electrons experience intra-band quantum excitation beyond the Fermi energy level (34).

For smaller size of the metallic nanoparticles, there is a small number of atoms that make the particle. This will reduce the potential attraction between the conduction electrons and metal ions of the particle, which leads to an increase in the conduction band energy. In the other hand, larger size of the metallic nanoparticles means there is more atoms that form the particle, thus increasing the potential attraction and then reduce the energy of the conduction band of the metallic nanoparticles (34).

- **Surface-Plasmon Resonance**

Surface plasmon resonance (SPR) is a resonance effect which happens as a result of the interaction between the incident photon and the conduction electrons of metal nanoparticles. The interaction depends on the morphology of the metal nanoparticles (size and shape).

When an electric field acts on a metal NP, the loosely bound electrons will be polarized. And a charge separation will occurs. The separation of charges causes a linear restoring force by the positively charged nuclei. As a result the valance electrons start oscillations on the material surface. If the frequency of the incident photon matches the natural frequency of the metallic electron oscillation against the restoring force of the nuclei, the resonance will happen (35). Figure.1 in Appendix A shows the SPR process.

Silver nanoparticles absorb and scatter light with remarkable efficiency. When the conduction electrons interact with the incident light at specific wavelengths, these electrons undergo a collective oscillation. Their strong interaction with light occurs because the conduction electrons on the metal surface undergo a collective oscillation when they are excited by light at specific wavelengths. This SPR phenomena makes the absorption and scattering intensities of Ag NPs to be much higher than identically sized non-plasmonic nanoparticles. The properties of Ag NPs can be changed when the particles size and shape were controlled (36).

- **Energy Band Gap**

The energy band gap can be defined as the difference between the valance band and conduction band. Its nature differs when the material changes from bulk structure to nanostructure due to the quantum confinement effect.

In the quantum confinement effects, the electrons described in terms of potential wells, energy states, valance and conduction bands, and energy band gaps. These quantum effects depends on the dimensionality of the system in nanoscale. Because this effects is just observed when the size of the particle is very small when compared to the electron wavelength. The confinement effects is related to the concept of restriction of the randomly motion of the electrons. So, the electrons will move in specific energy level (discrete levels), as shown in figure.2 in Appendix A. Moreover, a reduction of the

particle size to nanoscale causes an increase in the discreetness in the energy levels and the energy band gap of the material (24).

1.5.3 Morphological Properties

It is a study of the size and shape of the structure.

- **Size of Nanoparticles**

The physical and chemical properties of the nanoparticles are highly affected by the size of these NPs. The fast heating in the microwave-assisted synthesis method accelerates the reduction of the precursor which resulted in nanostructured with narrow sizes. A decrease in the size of nanoparticles causes an increase of the surface area which is related to the increase of the surface energy, and this make aggregations of the formed nanoparticles (37). The size of NPs affect the position of the SPR.

- **Shape of Nanoparticles**

Different shapes of nanoparticles can be formed by the microwave-assisted synthesis method. These shapes will directly change the nature of the surface-plasmon resonance curve. The number of maximum peaks in the SPR curve indicates the shape of these NPs. For example: the spherical nanoparticles will have a single surface-plasmon resonance band (37).

The optical properties of the nanomaterials (reflection, absorption, transmission and light emission) are highly affected with the electronic structure. This structure is dramatically changes for different morphologies because the electronic structure in nanomaterials are much dependent on surface atoms. The size effects on optical properties of nanomaterials arise from two main factors, these are the increase in the energy level spacing (quantum confinement effect) and surface plasmon resonance (24).

Due to the quantum confinement effect of the electrons in nanoparticles, these NPs react differently with light when incident on it compared to the bulk material. The reduction in dimensionality has the highest effect on the energies of the lowest unoccupied molecular orbit (the conduction band energy) and the highest occupied molecular orbital (the valance band energy). The optical properties like emission and adsorption happen when the electron transition occurs between these two energy bands. By changing the

size and shape of the nanoparticles, their emission wavelengths can differ from the UV through the visible to the near-infrared regions of the light spectrum (24).

1.6 Literature Review

Silver Nanoparticles (Ag NPs) have attracted a great deal of interest in recent years because of their special electrical, optical and morphological properties. Researchers used various methods to prepare it. Moreover, a lot of techniques were used to characterize these properties. Among these methods the Microwave-Assisted (MW) synthesis is the fastest and easiest one with successes in producing Ag NPs. A previous study which was done by Tetsushi Yamamoto et al.(12) used the MW method to prepare Ag NPs with size range $4.9 - 7.4$ nm by alcohol reduction of fatty acid silver salts under microwave irradiation for $1 - 5$ min at $413 - 430$ K. They controlled the size of NPs by changing length of the alkyl chains in the fatty acids. Angshuman Palm, Sunil Shah and Surekha Devi (4) used the MW method to produce spherical and monodispersed silver nanoparticles, they used ethanol as reducing agent and PVP as stabilizing agent. Highly monodispersed stable polycrystalline silver nanoparticles were obtained during a period of 5s. Soon Wei Chook et al. (38) fabricated Ag NPs and AgGo composites by MW method to study their antibacterial performance. The Ag NPs were distributed randomly on the surface of graphene oxide. Xuesen Hong et al. (39) prepared different shapes of Ag NPs: nanocubes, nanowires and nanospheres, via a MW method and characterized by UV-visible Absorption Spectroscopy (UV-vis), X-Ray Diffraction (XRD) and Transmission Electron Microscopy (TEM). Chengli Tang et al. (40) showed that the MW method can be applied to the production of conductive silver nano-ink which composed of multi-scaled NPs and a little number of nano-rods. The written tracks can have an electrical resistivity of $14.2\ \mu\Omega.cm$ with just $0.025\ mol\backslash L$ of silver contant. A comparison between synthesis methods of Ag NPs which done by Hayelom Dargo Beyene et al, (41) showed that the MW method is favorable among the different methods. It produces a higher concentration of Ag NPs rapidly compared to the others with the same temperature and exposure. Hossein Barani and Boris Mahltig (42) published a research in which fluorescent Ag NPs were prepared by the MW method, with trisodium citrate for both reducing and stabilizing agent. The effect of parameters such as reaction time, temperature, and trisodium citrate concentration (100, 200, and 400 ppm) were studied on the properties of synthesized Ag NPs. Furthermore,

Roberta Manno et al. (43) showed that The fast heating rate and volumetric character of MW heating were important for the synthesis of very small Ag NPs with a regular size distribution of (1.6 ± 0.7) nm, obtained after 17 s production duration. They conclude that increasing the temperature and time would give a lower homogeneity of the resulted product. In addition, a comparison done by K J SREERAM et al. (44) between conventional production methods (conventional temperature assisted process and controlled reaction at elevated temperatures) and microwave assisted process have been evaluated for the type of Ag NPs production. It has been shown that the MW process was faster and produced particles in the size of 12 nm. Different nanomaterials were synthesized using the microwave-assisted synthesis method. Ruthenium nanoparticles (Ru NPs) were synthesized in a small size $(2 - 5$ nm) using the MW method by Sakshi Gupta et al. (45) The Ru was used as a precursor which reduced by the glucose, with Polyethyleneglycol (PEG) as a stabilizing agent which protect the formed Ru NPs from aggregations. The size of the Ru NPs were controlled due changing the microwave power and irradiation time. They concluded that the size of NPs decreased when they decrease the irradiation time with an increase in the microwave power. A previous study done by Prasant Sutradhar et al.(46) success in the preparation of Aluminum nanoparticles (Al NPs) from Aluminum Nitrate by the microwave method. They used the extract of coffee and tea. The morphological and optical properties of these NPs were characterized using the Scanning electron microscope (SEM), UV-Vis absorption spectroscopy and Fourier transform infrared spectroscopy (FTIR). They obtained that the Al NPs are spherical in shape with average size of $(50 - 200$nm), the Surface-plasmon resonance band occurs at 271nm. No reducing agent and stabilizers use in the preparation process. Cobalt Oxide (Co_3O_4) nanoparticles were prepared using the microwave-assisted synthesis method by S. Vijayakumar et al. (47) Using the Tunneling electron microscope (TEM), the prepared NPs were analyzed. The average particle size is 24nm and the obtained Co_3O_4 NPs are homogeneous and well-distributed in size and shape, this is due to the uniform heating in the used microwave preparation process. The direct band gap was estimated from the absorbance values using Tauc's equation. Its value is approximately 2.43ev, which is larger than that for the bulk material. A. Kajbafvala et al. (48) succeeded in the preparation of Zin Oxide nanostructures (ZnO) using two different chemical solution methods by the simple microwave-assisted synthesis method. They produced large scale productions with high energy efficiencies.

The photocatalytic performance of the produced ZnO Nano powders was characterized using methylene blue (MB) photo-degradation with UV lamp irradiation. Two shapes of the ZnO were obtained: flower-like and spherical, with average size of 55nm and 28nm. The specific surface area was $22.9\, m^2/gr$ for the flower-like shape and $98\, m^2/gr$ for the spherical one. Both shapes has approximately the same energy band gap value. M. Iniya Pratheepa and M. Lawrence (49) published a research in which they prepared pure and cadmium-doped copper oxide (CuO) nanoparticles by the microwave-assisted synthesis method using copper acetate as the precursor. They obtained NPs with average size of $10-14$ nm for the pure CuO nanoparticles, and $42-87$nm for the doped CuO nanoparticles. These NPs were studied by X-ray diffraction, scanning electron microscope and energy-dispersive X-ray spectroscopy.

Different parameters could be changed during the preparation process: the power of the MW (medium-low (ML), medium (M), medium high (MH) and High (H)), the time of heating (30s and 90s) and the ratio of precursor to stabilizing agent ($1:1/2, 1:1, 1:2$ and $1:3$). The samples of Ag NPs will be analyzed using different techniques (Vector Network Analyzer (VNA), Ultra-Violet visible spectroscope (UV-vis) and Atomic Force Microscope (AFM)) and then make optimization to get the best sample. All measurements will be performed on solution form.

1.7 Applications of Silver Nanoparticles

Silver nanoparticles are used in several fields due to their especial physical, chemical, and optical properties. Some of these fields are summarized as the following points:

- Ag NPs is an anti-bacterial agent, which make it used widely in the health industry, food storage, and water treatment. The Ag NPs have the capability to overcome the resistance of bacteria to the antibiotic. This anti-bacterial agent property comes from the large surface to volume ratios and crystallographic surface structure of the Ag NPs compared to other nanomaterials (50). The Ag NPs were used successfully to avoid dental diseases, because these NPs have the ability to restrict Plaque biofilm formation, which is one cause of the dental diseases (51).

- Ag NPs has special electrochemical properties, so they take a place in several nanophysics applications:

1. Nanoscale sensors. This would produce lower detection limit and faster response time (52).

2. Ag NPs can be used as a good electromagnetic shielding material (52).

3. Ag NPs can be a good choice to enhance the properties of several materials (52).

4. Fabrications of Antennas: The fabricated Ag NPs conductors gives a very small electrical loss in the high frequency range. This will increase the opportunity of designing antennas in small sizes with high performance (53).

5. Electronically conductive adhesive: Due to the high conducting nature of the Silver nanoparticles, they can be used in the electrodes as a Silver paste. In addition, it can be used in electronically conductive adhesives (ECAs) as conductive fillers (53).

6. Solar cells optimization: The Ag NPs can be used in the interface between the metal and dielectric contacts in solar cells. This will improve the light-trapping properties of the Silicon solar cells because of the increase in the absorbance capacity and obtaining hot electrons which enhance the photocurrents in these solar cells (53).

- Diagnostics with Tunable Wavelength (54).

- Surface-Enhanced Fluorescence (54).

1.8 Research Objectives

The main goals of this thesis can be summarized as:

1. Prepare Silver nanoparticles (Ag NPs) samples by the Microwave-assisted synthesis method. Different parameters will be controlled via the synthesis process, this include the microwave power (ML, M, MH, and H), the microwave heating time (30s and 90s) and the precursor to stabilizing agent ratio ($1:1/2, 1:1, 1:2$ and $1:3$).

2. Study the morphological properties of the prepared Ag NPs using the Atomic Force Microscope (AFM). This include analyzing the size and shape of the samples.

3. Study the optical properties of the prepared Ag NPs using the Ultraviolet-Visible Absorption Spectroscopy (UV-Vis). This include analyzing the surface-plasmon resonance, the absorbance and the energy gap for each sample.

4. Study the electrical properties of the prepared samples using the Vector Network Analyzer (VNA). A check of the stability of the samples may be done.

This thesis is distinguished from the previous works in the same topic by its comprehensiveness. Different parameters will be controlled during this study, and each parameter set will be characterized using the advance characterization techniques.

Chapter Two

Methods and Calculations

2.1 Methodology

2.1.1 Materials

The Ag NPs were prepared by the microwave-assisted synthesis method. This method needs a precursor which is Silver Nitrate ($AgNO_3$) in this study. Ethylene Glycol was used as a reducing agent, and polyvinylpyrrolid (PVP) as a stabilizing agent.

All used materials obtained from Chemical Engineering Department Laboratories at An-Najah National University.

2.1.2 Preparation of Silver Nanoparticles

Several parameters were controlled during the preparation process. This include changing the microwave power, the microwave heating time and the precursor to the stabilizing agent ratio. The preparation of one sample done by adding the needed amount of the PVP gradually to 40 ml of Ethylene Glycol, they stirred magnetically using a magnetic stirrer at room temperature. After it totally dissolved, 0.17 gm of $AgNO_3$ added to the previous combination and again stirred magnetically.

The prepared solution was then placed in the microwave at the needed power for a given time. Modification of the microwave heating process is performed, a reflux was added to the microwave setup as shown in figure.3 in Appendix A. The reflux is an instrument which allows for facile heating of a solution, but without the loss of solvent that would happen from heating in an open vessel. In the reflux setup, solvent vapors are trapped by the condenser, and the concentration of reactants remains constant during the process (55). The color of the solution changed from a colorless to a yellowish one. This indicates the formation of Ag NPs. The color changed dramatically when changing the mentioned parameters above, these changes were shown in figure.1 (a),(b) and (c).

Figure 1

Color changes for the prepared Ag NPs samples. (a) 30s samples with different MW powers. (b) 90s samples with different MW powers. (c) Different $AgNO_3$: PVP ratios

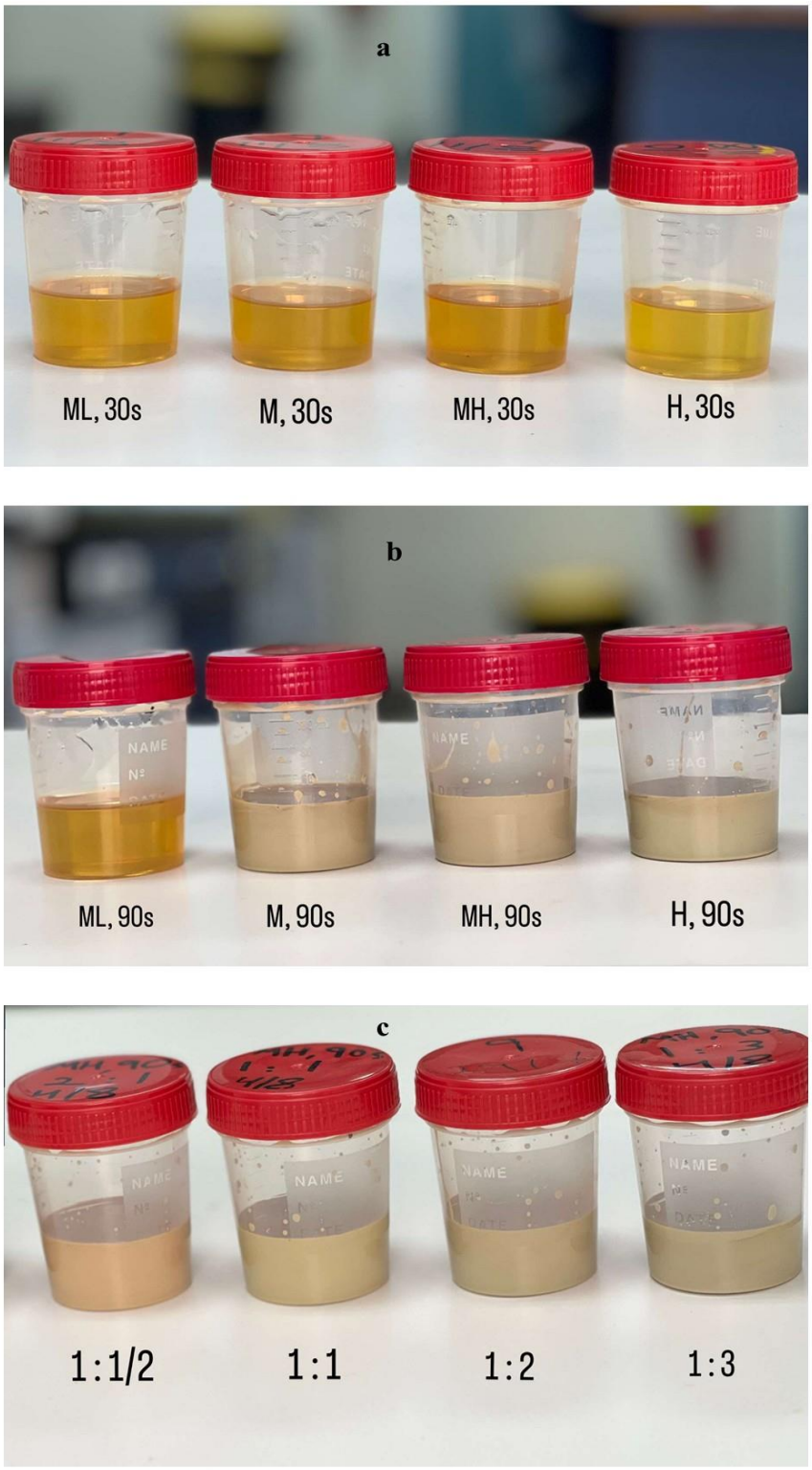

11 Samples were prepared in this study with different synthesis parameters, these samples were summarized due to preparation conditions in table 1.

Table 3

Summary of the synthesis parameters of the prepared Ag NPs samples

Sample number	Microwave power	Microwave heating time (s)	$AgNO_3$: PVP
1	ML	30	1 : 2
2	M	30	1 : 2
3	MH	30	1 : 2
4	H	30	1 : 2
5	ML	90	1 : 2
6	M	90	1 : 2
7	MH	90	1 : 2
8	H	90	1 : 2
9	MH	90	1 : 1/2
10	MH	90	1 : 1
11	MH	90	1 : 3

2.2 Data Collection and Analysis Methods

The Ag NPs will be characterized using different techniques according to the needed properties. Electrical, optical and morphological properties were studied using the Vector Network Analyzer (VNA), Ultra-Violet Visible (UV-Vis) Absorption Spectroscope and Atomic Force Microscope (AFM), respectively.

2.2.1 Vector Network Analyzer (VNA)

Material Research Lab at An-Najah National University. PLANAR R140 VECTOR REFLECTOMETER with frequency range 85 MHz-14 GHz and 50Ω impedance. The DAK Probe Stand has P/N: SM DAK 300AB, Switzerland.

One special feature of a VNA is that it contains both a source (which used to generate a known stimulus signal), and a set of receivers (one or more), used to find changes to this signal caused by the material under test. In summary, when the source provides a signal, it passes through the material under test.

Different types of vector network analyzer can be used. The principle of working differs according to how port the VNA has. For two ports VNA, when the signal injected to the material, both the signal that is reflected from the input boundary and the one which passes through to the output side of the material were calculated. While for the one-port

VNA, just the reflected electromagnetic wave was needed for analysis. Despite the type of the used VNA, the VNA receivers detect these obtained signals and compare them to the known stimulus one (56).

The used VNA can be defined as a high-precision dielectric parameter measurements (permittivity, conductivity, loss tangent) over the very broad frequency range from 200 MHz to 14 GHz for various applications in the electronic, chemical, food, and medical industries. It consists of a probe that is connected to a vector network analyzer (VNA) for measurement of the complex reflection coefficient (S_{11}) at the probe end. The measured S_{11} is then converted into the complex permittivity of the material under test using the DAK software (57).

The system uses advanced algorithms and novel hardware to measure the dielectric properties of liquids, solids, and semi-solids over a broad range of parameters. The measurement method is fast, reliable and non-destructive to the material under test (57). The material under test should satisfy some assumptions, it needs to be isotropic, homogeneous, and in a good contact with the coaxial probe (the contact is uniform and free of any air gaps or bubbles (58).

Once the VNA connected to the computer, the DAK program must be opened. First of all a calibration mode which is Open-Short-Load (O-S-L) was done. In this mode you make an open circuit which means the probe is connected to air, this followed by a short circuit by making a direct contact between the probe end and the copper strip which comes with the DAK package. Finally a load is connected to the probe, distilled water was used as a load in this study. After finishing the calibration process, the measurements can be done precisely.

The measurement step was done by connecting the prepared samples of the Ag NPs directly to the probe of the VNA, as shown in figure.2 (a) and (b), then click the measure ribbon in the menu bar. The data must be stored before finishing the measurements. The measured data which contains the dielectric properties of the material can export as an Excel file to the computer.

The VNA gives the values of complex permittivity, real and imaginary parts. They can be related by the complex relative permittivity equation as follows:

$$\varepsilon_r = \varepsilon' - j\varepsilon'' \tag{2.1}$$

In which the magnitude of the relative permittivity found from:

$$|\varepsilon_r| = \sqrt{\varepsilon'^2 + \varepsilon''^2} \tag{2.2}$$

The loss tangent can be calculated from the ratio between real and imaginary parts of permittivity

$$tan\delta = \frac{\varepsilon''}{\varepsilon'} \tag{2.3}$$

The impedance of the material under test depends on its dielectric properties. It is defined as:

$$Z_{in} = \sqrt{\frac{\mu_r \mu_0}{\varepsilon_r \varepsilon_0}} \tag{2.4}$$

μ_0 and ε_0 are the permeability and permittivity of free space, respectively.

By the approximation of a good conducting material (silver, Ag in our case), the real part of permeability $\mu' \approx 1$ and the imaginary part of permeability $\mu'' \approx 0$, which leads to the relative permeability, $\mu_r = 1$. (This assumption is assumed from the used VNA)

The impedance of air, Z_0 has a constant value:

$$Z_0 = \sqrt{\frac{\mu_0}{\varepsilon_0}} \tag{2.5}$$

The impedance matching rate can be calculated as the ratio between the impedance of the material under test (or the impedance at interface) and the impedance of free space:

$$\text{Impedance matching rate} = \frac{\text{Impedance at interface}}{\text{Impedance of free space}} = \frac{Z_{in}}{Z_0} \tag{2.6}$$

The reflection coefficient of the electromagnetic wave defined by:

$$R = \frac{Z_0 - Z_{in}}{Z_0 + Z_{in}} \tag{2.7}$$

The shielding effectiveness of the material can be described in the following form:

$$SE = -10\log(1 - R^2) \tag{2.8}$$

The penetration depth (or skin depth), can be calculated from:

$$\delta_s = \frac{1}{\sqrt{\pi f \mu_0 \mu_r \sigma}} \tag{2.9}$$

Where f is the frequency of the electromagnetic wave, and σ is the electrical conductivity of the tested sample which has been given from the VNA calculated data, or it can be calculated using this formula:

$$\sigma = \varepsilon_r \varepsilon_0 \omega \tan\delta \tag{2.10}$$

Where ω is the angular frequency and equals 2πf.

The attenuation constant of the electromagnetic wave inside the medium is the reciprocal of its penetration depth:

$$\alpha = \frac{1}{\delta_s} \tag{2.11}$$

2.2.2 Ultraviolet-Visible Absorption Spectroscopy

Laboratories of the Department of Mechanical and Chemical Engineering at An-Najah National University. UV-Vis absorption spectra for the Ag NPs solutions were recorded using a Beckman Coulter DU 800 Spectrophotometer in the region of 300-600 nm.

Ultraviolet and visible absorption spectroscopy is the measurement of the attenuation of electromagnetic radiation by an absorbing material. It can be used in material research for quantitative measurements and characterization of the optical properties of the material (59).

UV-Vis spectroscopy is based on the interaction between light and sample. When the light passes through or is absorbed by a molecule, it makes a vibration of that molecule. The wavelength of light that is most strongly absorbed by a molecule is called the maximum absorption wavelength (60). A schematic diagram of the working principle of UV-vis spectroscopy was shown in figure.4 in Appendix A.

When the incident photon hits a molecule and is absorbed, the molecule will excited and go to a higher energetic state. For the excitation process of the electron, the incident photon must have enough energy, this energy is called the band gap. The energy band gap equals to the difference of energy values between the highest occupied molecular orbital and the lowest unoccupied molecular orbital. These orbitals are also identified as the bonding and anti-bonding orbits. As the chemical structure differs from one molecule to another, the value of the energy band gap will also changes (61).

In this study, the prepared solutions which contains Ag NPs were investigated using the UV-Vis absorption spectroscopy. By taking a small amount of the samples and placing them on a distilled water, which we use as a reference in this process, the absorbance (A) of each sample was studied. The UV-Vis absorption spectroscopy gives the amount of light absorbed by the sample under measurements in a range of wavelengths ($300 - 600$ nm in our case). The used UV-Vis absorption spectroscopy was shown in Figure.2 (c).

The energy band gap (E_g), the needed energy for the electron to move from the valance band to the conduction band, can be calculated from the absorbance values which can be found from the UV-vis spectroscopy by using Tauc equation:

$$(ahv)^n = B\left(hv - E_g\right) \tag{2.12}$$

Where a is the absorption coefficient, h is Plank's constant, v is the frequency of the photon, n has a constant value of 2 for a direct band gap and ½ for indirect band gap, B is a constant and E_g is the energy band gap (62).

The absorption coefficient can be related to the absorbance value by Beer's law, so the values of (a) may be replaced by the obtained (A) values when finding the E_g.

By making a plot of $(ahv)^n$ on the Y-axix with hv on the X-axis, then make extrapolating along the linear region to the X-axis, the energy band gap can be estimated in electron volts (ev).

2.2.3 Atomic Force Microscopy

Faculty of Pharmacy Laboratories at An-Najah National University. Gwydion software was used for the analysis of Atomic Force Microscopy images. For AFM, a drop of a solution of Ag NPs was added onto mica substrates, dried under vacuum and analyzed by core AFM from Nanosurf Company, Switzerland.

Atomic force microscopy is the most flexible and powerful microscopy technology for studying samples at nanoscale. The AFM may be used to make images of the samples in three-dimensional topography, it also provides various types of surface measurements. It is powerful because the AFM can generate images with high accuracy (up to angstrom resolution), with minimum sample preparation (63).

The AFM slides were prepared by put a droplet of each sample on a solid slide, then put these slides in the oven for 1 hour.

The working principle of the Atomic Force Microscope can be summarized by three steps:

1. Surface sensing: The AFM uses a cantilever with a very sharp tip which scan over a sample surface. When the tip approaches the surface, the cantilever deflect towards the sample due to the close-range, attractive force between the surface and the tip. However, as the cantilever becomes even closer to the surface and makes contact with the tip, increasingly repulsive force takes over and causes the cantilever to deflect away from the surface (63).

2. Detection method: Cantilever deflections towards or away from the surface have been detected using a laser beam. The incident beam of the top of the cantilever has been reflected. So, any cantilever deflection will make changes in the reflected beam. These changes can be tracked by using a position-sensitive photo diode (PSPD) (63).

3. Imagine: The AFM images the topography of a sample surface by scanning the cantilever over a region of interest. The height of the tip above the surface may be controlled using a feedback loop, this make sure that we have a constant laser position (63).

Several abilities can be achieved using the Atomic force microscope:

1. Force Measurement: AFMs can be used to measure the forces between the needed sample and the probe of the device. These forces can be measured as a function of the mutual separation between the probe and the sample. From these forces different mechanical properties of the sample can be found (sample's Young's modulus and stiffness) (64).

2. 3D topography of the samples: From the interaction between the probe and the forces which the sample makes it, a 3D image of the sample can be taken. This is happened by scanning the position of the sample with respect to the AFM tip. The height of the tip will also be detected (64).

3. Manipulation: The properties of the material under test can be modified by using the forces between the sample and the probe of the AFM in a controlled manner (64).

After making the images of the prepared samples of Ag NPs using the AFM, the obtained results were modified using Gwyddion program. A histogram obtained for each sample, this show the average size of the prepared Silver nanoparticles.

Gwyddion is a modular program for the visualization and analysis of the scanning probe microscopy (SPM) data. Different measurement techniques can be analyzed using the Gwyddion program, this include the data taken from (AFM, STM). Several SPM data formats were supported by this program.

Gwyddion gives a large number of data processing functions, this include all the standard statistical characterization, data correction and levelling, grain marking or filtering functions. The program also have a number of specific, uncommon, odd and experimental data processing processes which may be useful for the analysis of the data (65).

The shape and size of the Ag NPs were studied. The used AFM was shown in figure.2 (d).

The parameters that have been used in the calculation were listed in table.4

Table 4

Numerical parameters used in calculations

Parameter	Numerical value
$\boldsymbol{h}$	6.62×10^{-34} J. s
$\boldsymbol{c}$	$3 \times 10^{8} m/s$
$\boldsymbol{\varepsilon_0}$	$8.85 \times 10^{-12} F/m$
$\boldsymbol{\mu_0}$	$4\pi \times 10^{-7} N/A^2$
$\boldsymbol{Z_0}$	376.7 Ω
$\boldsymbol{\pi}$	3.14
$\boldsymbol{e}$	2.71828
$\boldsymbol{n}$	2 for direct band gap ½ for indirect band gap

Figure 2

The used instruments in the characterization process. (a) and (b) show the VNA. (c) shows the UV-Vis absorption spectroscopy. (d) shows the AFM

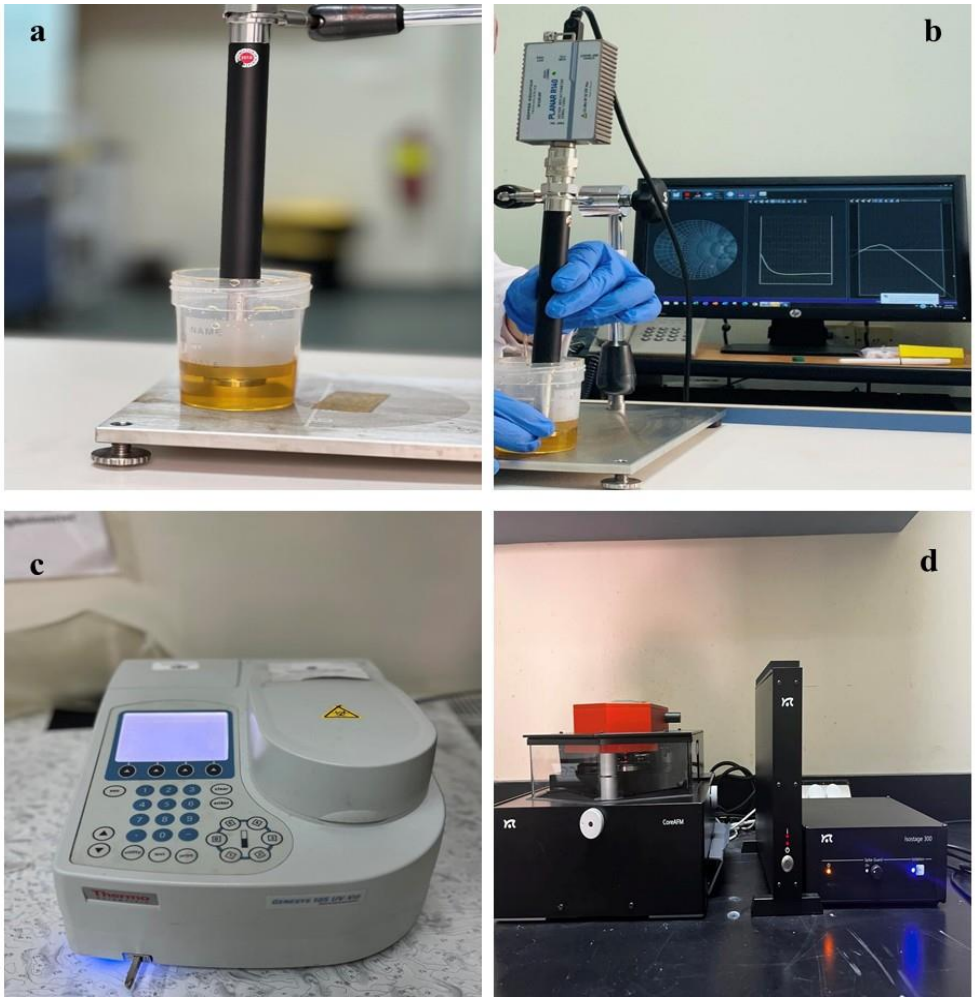

Chapter Three

Results and Analysis

In this chapter, the obtained results and an analysis of each were discussed. The morphological, optical and electrical properties of the prepared Ag NPs samples were studied using the mentioned analysis techniques, AFM, UV-Vis, and VNA, respectively. The studied parameters are compared for the samples of different powers (ML, M, MH, and H), different times (30s and 90s), and different $AgNO_3$ to PVP ratios ($1:\frac{1}{2}, 1:1, 1:2$ and $1:3$).

In the synthesis process, the Ethylene glycol used as a solvent and a reducing agent, which reduced the Ag ions from the precursor which is Silver Nitrate. The stabilizing agent was used to protect the formed Ag NPs from aggregations. The size of the prepared Ag NPs may be affected by the PVP amount.

3.1 Morphological Properties of Ag NPs

Atomic force microscope has been used to analyze the prepared Ag NPs samples. The shape and histogram of these NPs were shown in figure.3. The prepared Ag NPs has a spherical shape which does not affected by the different controlled parameters. But the size of these Ag NPs differs between samples. Figure.3 (a) shows the Ag NPs prepared at M microwave power for 90s, the size of the NPs has a range of $20-50$ nm. Increasing the microwave power to MH, with the same microwave heating time (90s), makes an increase in the range of the Ag NPs size. From figure.3 (b) It becomes in the range of $30-55$ nm (66). The Ag NPs which prepared at MH microwave power for 90s microwave heating time with $1:3$ ratio was represented in figure.3 (c), these NPs are in the size range $15-40$ nm. Decreasing the PVP ratio leads to more aggregations of the formed Ag NPs, which as a result cause an increase in these NPs size. Studying the results of figure.3 (d, b, c) with different ratios, we notice that increasing the PVP from ½ to 2 to 3 with respect to $AgNO_3$ decreases the NPs size range (67). To study the effect of microwave heating time on the Ag NPs size, figure.3 (e) which contains the Ag NPs synthesized at MH microwave power for 30s was compared with figure.3 (b). The 30s sample has Ag NPs with size range of $5-20$ nm (68).

Figure 3

AFM representation of Ag NPs and the corresponding histogram. (a1) for M power for 90s, (b1) MH power for 90s, (c1) 1:3 ratio, (d1) 1:1/2 ratio, and (e1) MH power for 30s

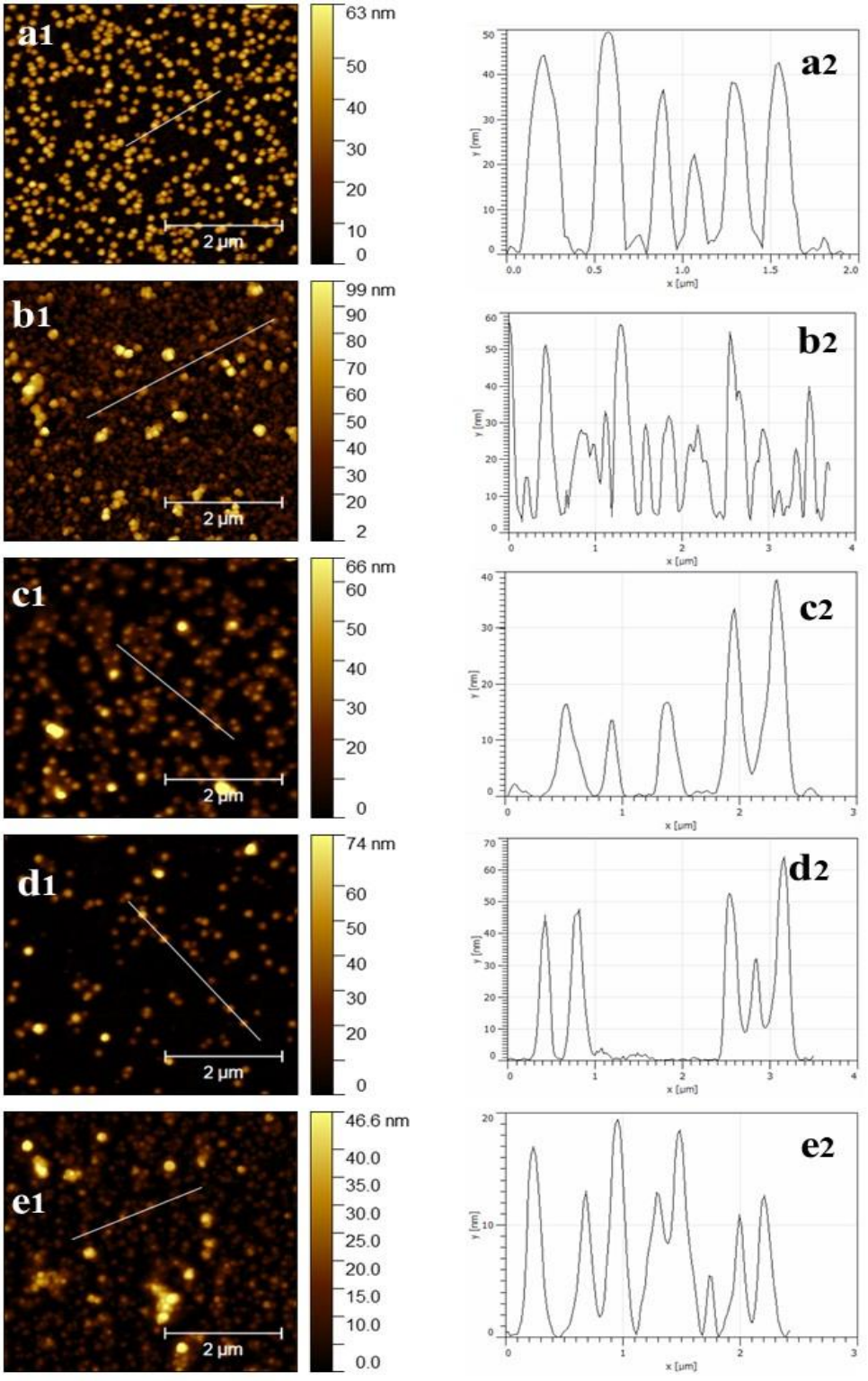

3.2 Optical properties of Ag NPs

3.2.1 Surface-Plasmon Resonance

After the preparation of the Ag NPs samples, the optical properties were studied using the UV-vis absorption spectroscopy. The maximum absorption wavelength peak (surface Plasmon resonance band) and the normalized absorbance values for each sample were detected. For the successful preparation of the Ag NPs we expect to have a maximum absorption wavelength peak approximately between 400 and 450 nm (69). The presence of one dipole surface-plasmon resonance peak in the absorption spectrum confirms the spherical morphology of the prepared Silver nanoparticles, which satisfied with the AFM results which show that all samples have spherical shape (70).

In figure.4 (a), the Ag NPs were successfully synthesized for 90s microwave heating time samples at all microwave powers which indicated from the SPR peak which is in the expected region. The SPR band is approximately 430 nm. An increase in the microwave power leads to a red shift of the SPR (towards the longer wavelengths) and becomes wider (70). The increase in the peak width is satisfied with increasing the Ag NPs size which happens when the microwave power increased.

Figure.4 (b) shows the effect of changing microwave heating time on the absorbance spectrum of the synthesized Ag NPs. Two samples with the same microwave power (MH) and ratio (1: 2) but different microwave heating time (30s and 90s) were compared. The Ag NPs were successfully synthesized for both 30s and 90s MW heating time samples which indicated from the SPR peak which occurs in the expected range. The SPR band is approximately 420 nm for the 30s sample. While the 90s sample has a SPR value of 428 nm. An increase in the MW heating time leads to a red shift of the SPR and becomes wider (42). This wider peaks satisfy with the larger size of the 90s sample over the 30s sample. So, the increase in the MW heating time causes an increase in the Ag NPs size which as a result causes this red shift and the peak becomes wider.

The effect of changing the $AgNO_3$: PVP ratio on the SPR peak was shown in figure.4 (c). It is obvious that all ratios can be used to synthesize Ag NPs. A decrease in the PVP ratio causes a red shift of the SPR towards the higher wavelengths and becomes slightly wider. When the ratio changes from 1: 3 to 1: ½ the SPR increased from 424 nm to

438 nm. Decreasing the PVP ratio make aggregates of the Ag NPs, which leads to a higher Ag NPs size. As a result a red shift and wider peaks will happen for the SPR.

3.2.2 Energy Gap

The energy gap was calculated from the mentioned Tauc equation, and by extrapolating the linear curve along the X-axis, the value of E_g may be estimated.

Figure.4 (d), (e) and (f) show the Tauc's plot for a direct band gap, by plotting $(ahv)^2$ against (hv) in electron volt, the E_g values can be estimated from the extrapolating of the linear region of the curves along the X-axis. In Figure.4 (d), by increasing the microwave power for the 90s samples, the value of E_g decreased from 2.75 ev to 1.97 ev. This decrease in the band gap might be due to the increase of the Ag NPs size which happens because of the increase in the MW power. From equation (1.2), a red shift that occurs when increasing the microwave power (higher λ_{max}) corresponded to lower conduction band energy, which causes a reduction in the energy band gap value.

In figure.4 (e), the increase in the microwave heating time from 30s to 90s causes a decrease in the $E_g$value from 2.5 ev to 1.9 ev. This decrease in the band gap might be due to the increase of the Ag NPs size which happens because of the increase in the MW heating time.

The value of the energy band gap is also affected by the $AgNO_3$: PVP ratio. This effect is represented in figure.4 (f), decreasing the PVP ratio makes a decrease in the energy band gap. In our case it decreased from 2.12 ev to 1.86 ev. This occurs because of the bigger size of Ag NPs with lower PVP ratios which resulted in a decrease of the energy gap values.

The energy band gap is highly affected by the morphology of the silver nanoparticles. An increase in the particle size causes a decrease in the energy band gap (71), (47). The theoretical value of the direct band gap of the Ag NP is 2.51ev (72). Which is approximately the same as its value in this study.

Figure 4

(a), (b) and (c) show the absorbance spectrum. (d), (e) and (f) show the Tauc's plot for the Ag NPs. (a) and (d) represent different MW powers for 90s. (b) and (e) for different MW heating times. (c) and (f) for different $AgNO_3$: PVP ratios

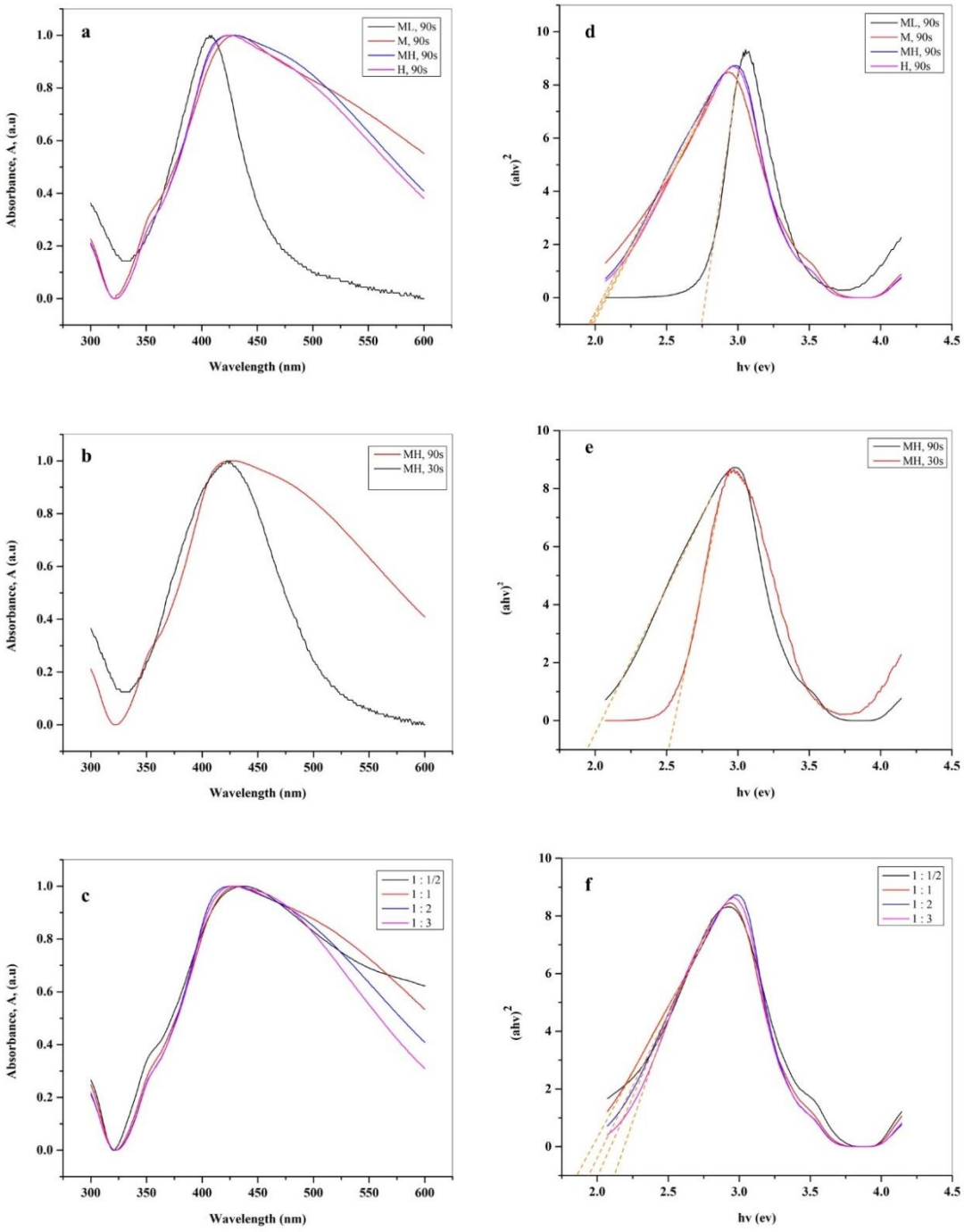

3.3 Electrical properties of Ag NPs

In this section, the electrical conductivity, real and imaginary parts of permittivity, loss tangent, impedance matching ratio, penetration depth (or skin depth), attenuation constant, reflection coefficient and shielding effectiveness were analyzed for the prepared Ag NPs samples in a frequency range ($2-14$ GHz) at room temperature using the VNA. Several synthesis conditions were controlled when calculating each mentioned parameter.

3.3.1 Electrical Conductivity

Figure.5 shows the electrical conductivity of the Ag NPs samples with different controlled synthesis parameters. Figure.5 (a) represent Ag NPs with different microwave powers (ML, M, MH and H) for 90s microwave heating time. For the H microwave power and 90s Ag NPs sample, the value of σ increased from 1.9 s/m to 3.1 s/m when the frequency changed from $2-7$ GHz, then it approximately has a constant value up to 14 GHz. This behavior is the same for all microwave power.

An increase in the MW power leads to higher values of σ. At $f = 8$ GHz, the electrical conductivity increased from 2.9 s/m to 3.1 s/m for the 90s samples when changed from ML to H power. This can be understood by the fact of increasing the size of Ag NPs when the microwave power increased, this leads to an increase in the electrical conductivity values (73).

Figure.5 (b) represents the effect of changing microwave heating time on the electrical conductivity value when the microwave power is constant (MH). The increase in the MW heating time leads to a big enhancement of the σ values. σ is approximately zero for the 30s sample if it compared to the 90s sample. This can be related to the bigger size of the Ag NPs obtained from the AFM in the 90s sample than that of the 30s sample.

It is important to show that the 30s samples with different MW powers give unstable measurements of the electrical conductivity. So, no more electrical properties needed to analyzed for the 30s Ag NO_3 samples. This is shown in Figure.5 in Appendix A.

Figure.5 (c) indicates the behavior of the electrical conductivity in the frequency range $2-14$ GHz when the PVP ratio is changed (with constant power and time, MH and 90s). Its value increased linearly from $2-6$ GHZ, then its value is approximately constant. At $f=8$ GHz, the value of σ increased from 2.3 s/m to 3.8 s/m when the ratio differs from $1:3$ to $1:1/2$.

An improvement in the electrical conductivity of the Ag NPs samples can be satisfied by either increasing the MW power, the MW heating time or decreasing the Ag NO_3: PVP ratios. The effect of increasing the microwave heating time from 30s to 90s is the largest among the controlled conditions.

3.3.2 Real and Imaginary parts of permittivity

Figure.6 (a), (b) show the real part of the complex permittivities (ε') in the frequency range $2-14$ GHz. Figure.6 (a) represents $\varepsilon'$of the four different MW powers (ML, M, MH, and H) for 90s microwave heating time. Its values were decreased dramatically in the whole frequency range, for the H microwave power and 90s its value decreased from 18.4 to 5.2. Moreover, an increase in the microwave power causes a slightly increase in ε'. In the middle of the frequency range, at $f=8$ GHz, ε' increased from 5.4 to 5.9 when the microwave power increased from ML to H for the 90s samples.

In Figure.6 (b) there is an obvious differences in ε' values between the different PVP ratios. The higher PVP ratio corresponding to the lowest value of ε'. At 8 GHz its value increased from 5 to 6.8 when the PVP ratio changed from $1:3$ to $1:1/2$ (All samples prepared at MH and 90s in this case).

Figure.6 (c) shows the imaginary part of the complex permittivities (ε'') for different microwave power samples for 90s microwave heating time. It can be seen that its value is dramatically decreased in the whole frequency range, for the H microwave power and 90s its value decreased from 16.7 to 3.9. The increase in MW power cause a slightly increase in the ε'' value. At $f=8$ GHz, for the 90s samples, ε'' increased from 6.6 to 7 when the microwave power increased from ML to H.

The imaginary part of complex permittivities (ε'') for different PVP ratios has shown in Figure.6 (d), there is a dramatically change in its value due to the change of PVP ratio. At $f=8$ GHz its value changes from 5.1 to 7.8 when the ratio changes from $1:3$ to

$1:1/2$. The differences between the curves are higher for the low frequency range than the high frequency range.

As a result, to enhance the material charge storage property the microwave power needs to be higher and the PVP ratio should be lower (22). This concluded from the higher values of ε' for 90s Ag NO_3 sample with H microwave power, and $1:1/2$ ratio. In addition, the same conditions makes an improvement in the dielectric attenuation performance of electromagnetic wave due to the improved values of ε''. It's clear that the effect of changing the PVP ratio is better than changing the MW power for the enhancement of the dielectric properties.

3.3.3 Loss Tangent

Figure.7 (a) and (b) represent the loss tangent values calculated for the Ag NPs as a function of frequency. Figure.7 (a) shows the electric loss tangent for the Ag NPs which was prepared for 90s MW heating time, with different microwave powers (ML, M, MH, and H). It is almost constant between 4-6GHz, then decreases from 6 to 14 GHz. This indicates that the largest attenuation of the electromagnetic wave when it passing through the Ag NPs occurs at 6 GHz.

An increase in the MW power leads to slightly decrease in the dielectric loss of the Ag NPs samples (22). The highest loss tangent occurs for the ML sample.

In figure.7 (b) the loss tangent for different Ag NPs samples which all prepared at MH power for 90s, but with different PVP ratios ($1:1/2, 1:1, 1:2$ and $1:3$) were plotted as a function of frequency. It is clear that there is a wide peak which satisfy the highest attenuation, this peak ranging from $2.5-6.5$ GHz. The Ag NPs sample which prepared at MH power for 90s and with $1:2$ ratio has the largest value of $tan\delta$ which is about 1.2.

Figure 5

The electrical conductivity was shown as a function of frequency for (a) different MW powers. (b) different MW heating time. (c) different $AgNO_3$: PVP ratios

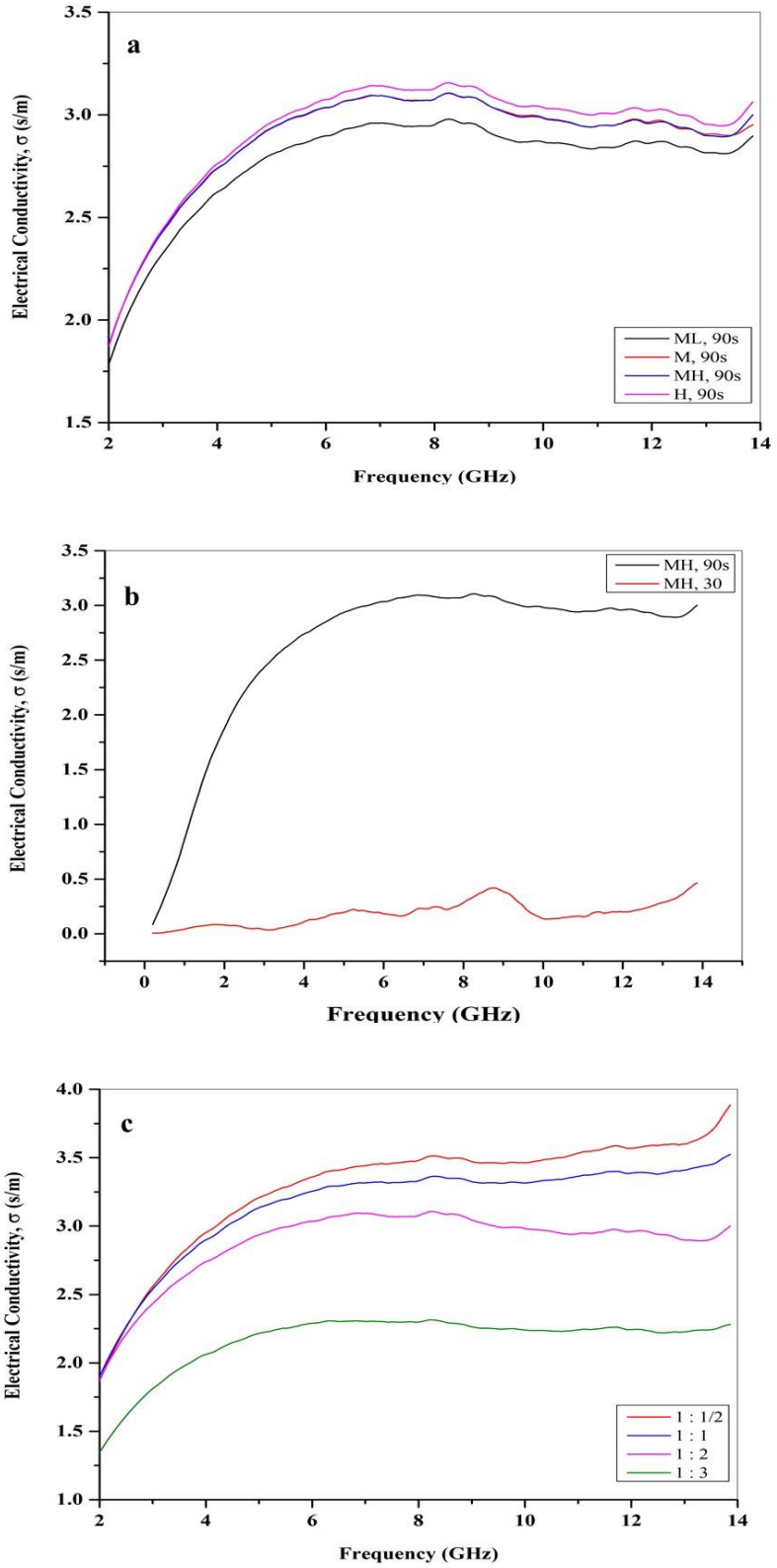

Figure 6

Real and imaginary parts of complex permittivity as a function of frequency. (a) and (c) represent $\boldsymbol{\varepsilon'}$ *and* $\boldsymbol{\varepsilon''}$ *for different MW powers. (b) and (d) represent* $\boldsymbol{\varepsilon'}$ *and* $\boldsymbol{\varepsilon''}$ *for different* $AgNO_3$*: PVP ratios*

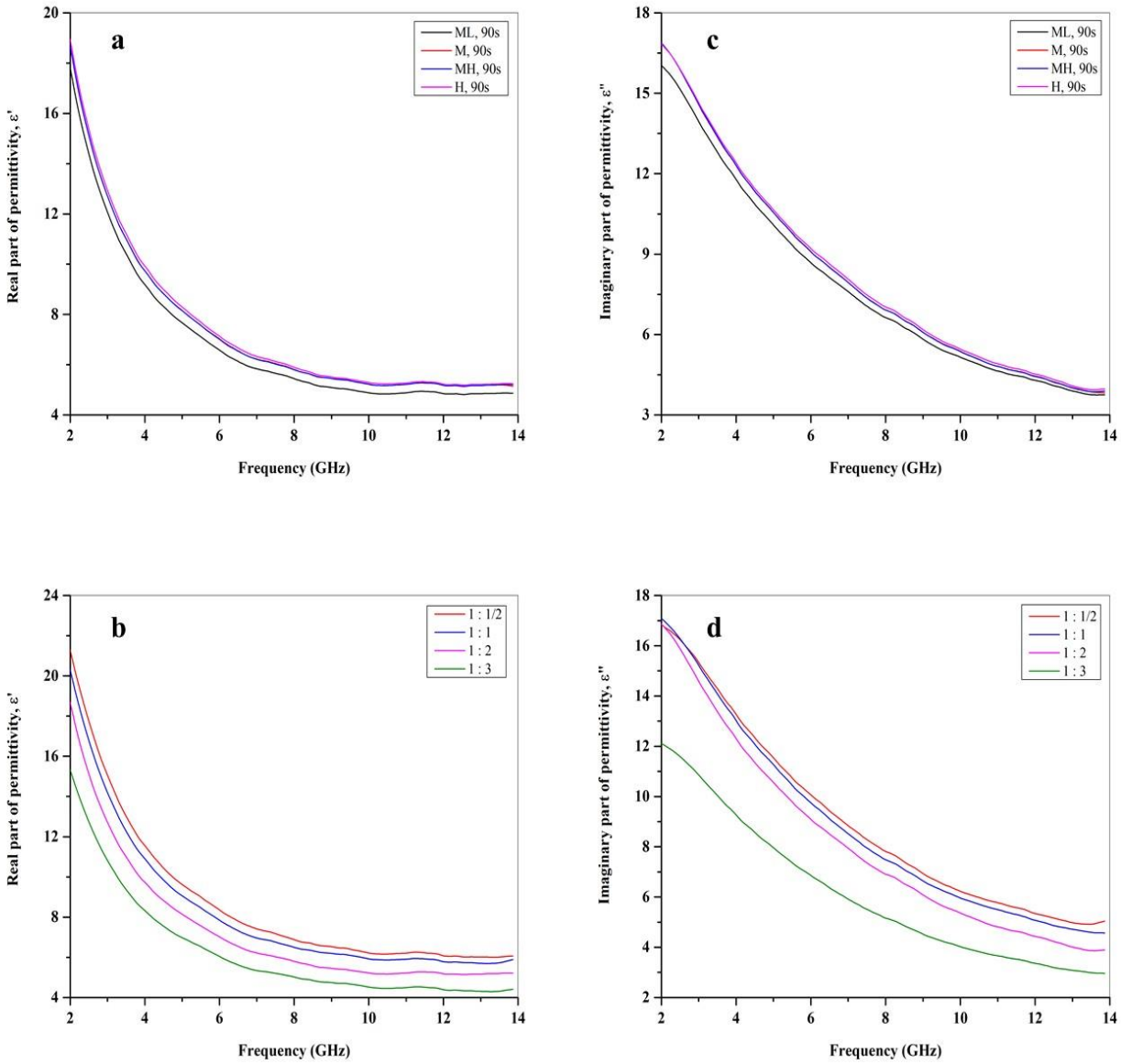

Figure 7

The loss tangent as a function of frequency. (a) Shows $\boldsymbol{tan\delta}$ *for different MW powers. (b) Shows* $\boldsymbol{tan\delta}$ *for different* $AgNO_3$*: PVP ratios*

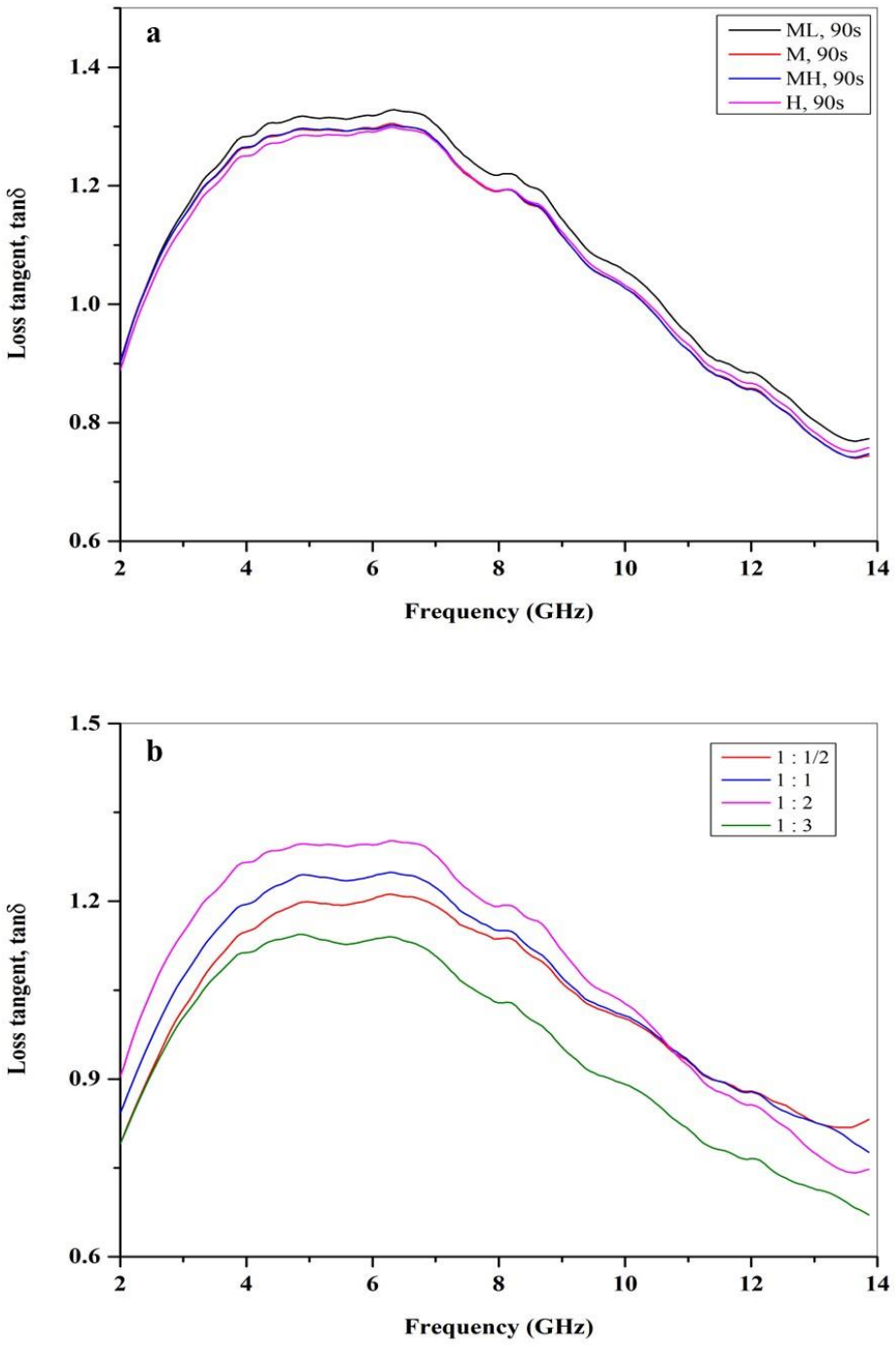

3.3.4 Impedance Matching Ratio

In the previous chapter, the relation of the impedance of the samples was shown. It depends on the relative permittivity and relative permeability values of the material. The impedance matching rate was defined as the ratio between the impedance at interface (Ag NPs samples in this study) and the impedance of air, which has a constant value. From the obtained values of relative permittivity, and by the approximation of the relative permeability to be 1, the values of Z was calculated for the synthesized Ag NPs at each frequency point. Then these values were divided into the impedance of air to get $Z/Z0$.

Figure.8 (a) and (b) shows the value of the impedance matching ratio as a function of frequency. For all Ag NPs samples, it increased linearly in the used frequency range ($2-14$ GHz). Figure.8 (a) studied the effect of the increase in the microwave power on the impedance matching ratio (at constant microwave heating time 90s). It is clear that the impedance matching ratio reduced gradually with increasing the MW power for the 90s Ag NPs samples. In Figure.8 (b) the decrease of PVP ratio caused a decrease in the impedance matching ratio. For example, at $f = 8$GHz, when the ratio decreased from $1:3$ to $1:1/2$ the impedance matching ratio changed from 0.37 to 0.31. The effect is much clear for the higher frequency values.

The impedance matching ratio for a good absorbing material should be greater than 0.3 to let incident microwave efficiently enter the absorbers with little reflections (74). The $1:1/2$ ratio of the Ag NPs sample reaches this value (0.3) at approximately $f = 7.4$ GHz while the $1:3$ ratio reaches it at $f = 4.7$ GHz. From that we concluded that the $1:3$ ratio is better than $1:1/2$ ratio for the absorbing material applications, because the $1:3$ ratio has a wide range of frequency ($4.7-14$ GHz) with impedance matching ratio larger than 0.3.

These results indicate that the increase of MW power and decrease in the PVP ratio would have an adverse effect on the impedance matching performance of the absorber which was more obvious in the high frequency range with higher electromagnetic energy.

Figure 8

The Impedance matching ratio as a function of frequency. (a) Shows Z/Z_0 for different MW powers. (b) Shows Z/Z_0 for different $AgNO_3$: PVP ratios

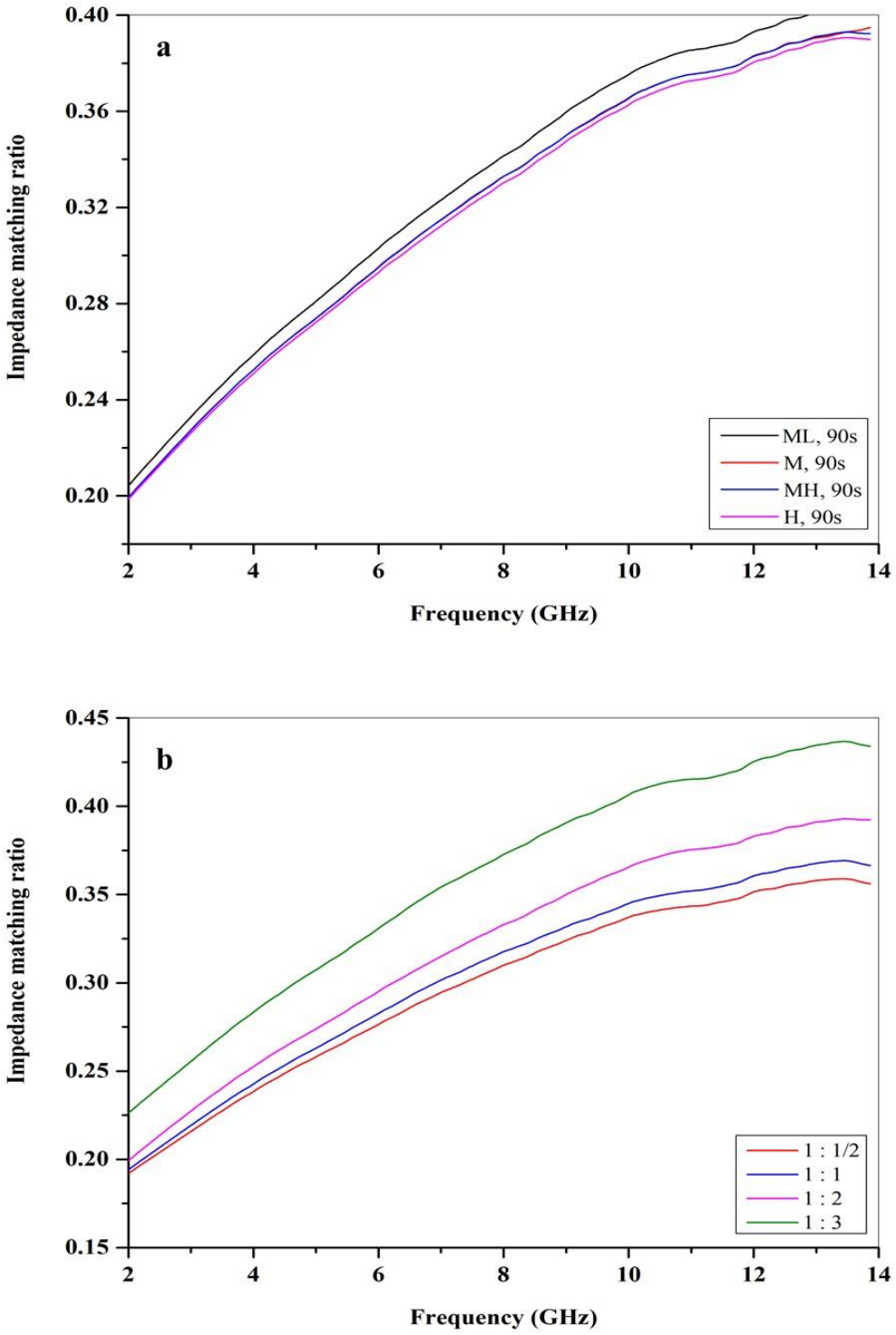

3.3.5 Penetration Depth (Skin Depth)

The penetration depth value was calculated from its relation which was mentioned previously. It depends on the electrical conductivity of the sample, its relative permeability (considered to be $= 1$ in our case), and the value of the frequency at which the data was taken. Figure.9 (a) and (b) shows the penetration depth in which the electromagnetic wave attenuate to 37% of its initial value when passing through the sample as a function of frequency.

All plots indicate that δ_s has an exponential decrease when the frequency increased from $2 - 14$ GHz. Figure.9 (a) represents the effect of changing the microwave power on δ_s value for 90s microwave heating time. It is clear that the higher microwave power leads to a slightly decrease in δ_s. At $f = 8$ GHz, when the microwave power increased from ML to H, the value of δ_s decreased from 3.3mm to 3.1mm.The decrease of δ_s is highly affected with decreasing the PVP ratio. Figure.9 (b) shows that at $f = 8$GHz, δ_s decreased from 3.7mm to 3mm when the ratio changed from $1:3$ to $1:1/2$.

For better attenuation, the Ag NPs samples with $1:1/2$ ratio can be used successfully, in which the incident electromagnetic wave will reduced into 37% of its initial value just in 3mm depth inside the material.

3.3.6 Attenuation Constant

The higher attenuation constant indicates that the material is better to attenuate the electromagnetic wave passing through it, it was calculated from the reciprocal of the penetration depth at each frequency point. From figure.10 (a) and (b) it can be achieved by increasing the MW power or decreasing the PVP ratio.

Figure.10 (a) indicates that increasing the microwave power will increase the attenuation constant value. At $f = 8$ GHz, the attenuation constant will increase from 307db/m to 316db/m when the microwave power increased from ML to H for 90s microwave heating time.

The effect of decreasing the PVP ratio is much clear than changing the power of the microwave, Figure.10 (b) shows that at $f = 8$GHz, α increased from 270.7 db/m to 333.2 db/m when the $AgNO_3$: PVP ratio changed from $1:3$ to $1:1/2$. In the whole

frequency range ($2-14$ GHz), the attenuation constant increased linearly with frequency.

3.3.7 Reflection Coefficient

The reflection coefficient measures the amount of electromagnetic wave reflected when passing through the material with respect to the original incident wave. In Figure.6 (a) and (b) in Appendix A, it's obvious that the reflection coefficient exponentially decreased in the frequency range ($2-14$ GHz) for all Ag NPs samples. Figure.6 (a) represents the effect of changing microwave power on the reflection coefficient value for 90s Ag NPs samples. An increase in the microwave power leads to a slightly increase in the R value especially in the higher frequency values. At $f = 8$GHz, R increased from 48% to 50% when the microwave power changed from ML to H.

The effect of changing the $AgNO_3$: PVP ratio was analyzed in figure.6 (B), decreasing the PVP ratio make an improvement in the R value in the whole frequency range. At $f = 8$ GHz, R increased from 45% to 52% when the ratio decreased from $1:3$ to $1:1/2$.

The highest reflection coefficient obtained when the Ag NPs prepared at MH power for 90s, with $1:1/2$ ratio. This is satisfied at the whole frequency range. This is related to the higher value of electrical conductivity of this Ag NPs sample.

3.3.8 Shielding Effectiveness

Shielding effectiveness is related to the reflection coefficient values, the more electromagnetic wave reflected by the material means this material is a good shielding material. Figure.7 (a) and (b) in Appendix A indicate that the SE value decreased exponentially in the used frequency range ($2-14$ GHz) like the R curves. The effect of changing microwave power and changing the $AgNO_3$: PVP ratio is the same for SE and R values. In addition, the ratio effect is clearer than the MW power. At $f = 8$ GHz, the SE value increased from 1.1 db to 1.3 db when the power increased from ML to H for the 90s Ag NPs samples. At the same frequency point, its value increased from 1 db to 1.4 db when the ratio changed from $1:3$ to $1:1/2$. The best Ag NPs sample for shielding applications obtained when synthesized at MH power for 90s with $1:1/2$ ratio.

Figure 9

The penetration depth as a function of frequency. (a) Shows $\boldsymbol{\delta_s}$ *for different MW powers. (b) Shows* $\boldsymbol{\delta_s}$ *for different* $AgNO_3$*: PVP ratios*

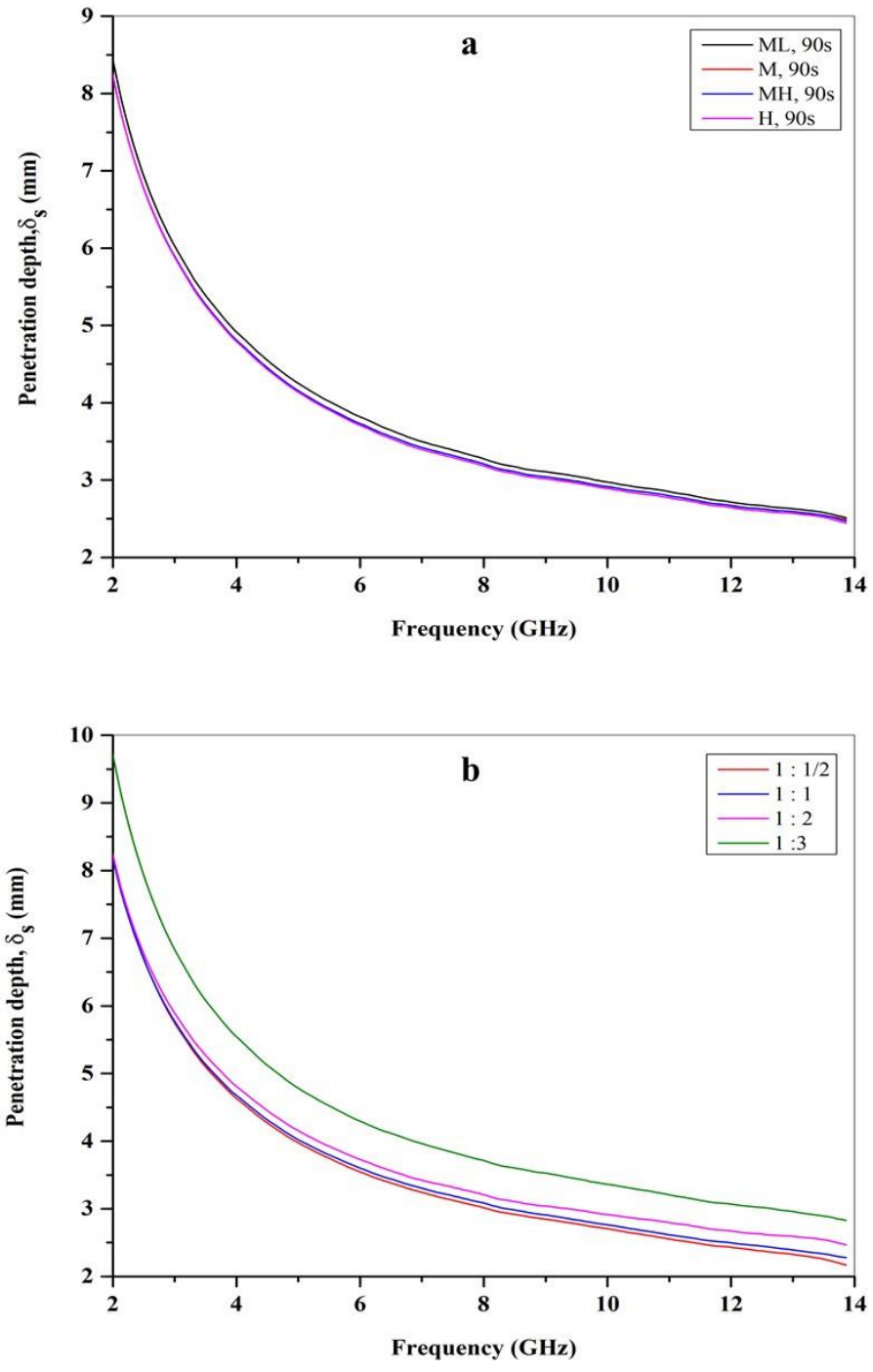

Figure 10

The attenuation constant as a function of frequency. (a) Shows $\boldsymbol{\alpha}$ *for different MW powers. (b) Shows* $\boldsymbol{\alpha}$ *for different* $AgNO_3$*: PVP ratios*

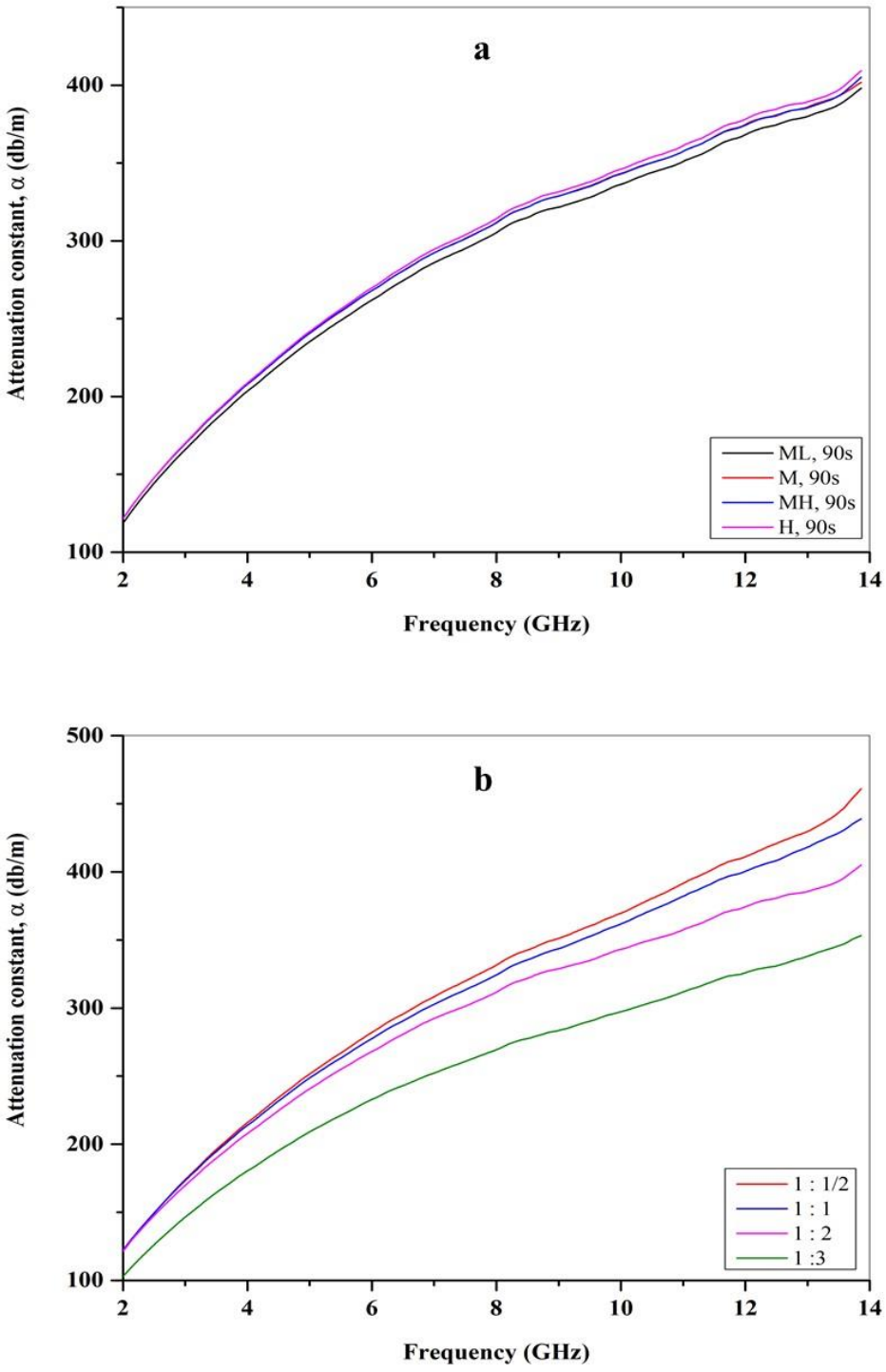

3.4 Yield of Silver Nanoparticles

The yield can be defined as a measure of the quantity of the product formed in the chemical reaction, with respect to the consumed amount of the reactant. A high yield means larger amount of the product obtained (75). The percentage yield calculated from the ratio between theoretical and actual yield. Where the theoretical is the maximum amount of the product that can be formed in a given reaction, and the actual yield is the obtained amount in the experimental work (75).

We try to calculate the yield of Ag NPs in each sample (4-samples with different powers for 90s microwave heating time). This happens by putting 10 ml from each solution sample in a small container and heating it on the hot plate until all the solution evaporate, the left will be a combination of Ag NPs and PVP. This process was shown in figure.8 in Appendix A.

We weight each container when it is empty and after the evaporation of the solution. Taking the exceeded weight (which comes from 10 ml of the sample). Multiplying by 4 to get this for the whole sample (40 ml). Dividing by the initial used quantity of Ag NPs and PVP (= $0.17\ gm + 0.34\ gm = 0.51\ gm$).

The yield is calculated by dividing the last calculated number on 0.51 (the initial amount of sample when the ratio of $AgNO_3$: PVP = 1: 2). The obtained values were mentioned in table.5.

Table 5

Yield calculations for 90s Ag NPs samples

Ag NPs sample	ML, 90s	M, 90s	MH, 90s	H, 90s
Weight of empty container (gm)	14.1799	12.5710	13.5984	13.9573
Weight of the container after evaporation (gm)	14.2523	12.6408	13.6722	14.0270
The exceed weight for 10ml solution (gm)	0.0724	0.0698	0.0738	0.0697
The exceed weight for 40ml solution (gm)	0.2896	0.2792	0.2952	0.2788
The yield	56.78 %	54.75 %	57.88 %	54.67 %

From table.5 it is clear that the yield of Ag NPs is approximately not affected with changing the microwave power for the 90s microwave heating time.

3.5 Limitations

In the preparation process, Ag NPs with 60s microwave heating time were synthesized (with four different microwave powers). These prepared nanoparticles were characterized using the different characterization technique (UV-Vis, and VNA).

Unexpected results were obtained for this microwave heating time samples. One of these result, the electrical conductivity which gives an inverse behavior from the expected one. And repeating the measurements different time give different values, which indicates that these Ag nanoparticles are not stable.

Sometimes increasing the microwave power leads to a decrease in the electrical conductivity values. Another times, a random behavior of the electrical conductivity values with different microwave powers were obtained. This was represented by figure.9 (a) and (b) in Appendix A.

All these results says that the 60s microwave heating time is not suitable for the preparation of Silver nanoparticles by the microwave-assisted synthesis method.

A comparison between some samples of the prepared Ag NPs were found in table.6. Morphological, optical and electrical properties of each Ag NPs sample were founded. The electrical properties all calculated at $f = 8GHz$).

The electrical properties of the 30s Ag NPs samples were not analyzed because of the unstable behavior of these samples electrical conductivity.

Table 6

Properties of some Ag NPs samples (electrical properties at f=8GHz)

	M, 90s	MH, 90s	1: 3	1: ½	MH, 30s
Average size (nm)	$20-50$	$30-55$	$15-40$	$30-65$	$5-20$
Shape	Spherical	Spherical	Spherical	Spherical	Spherical
SPR (nm)	425	430	423	436	419
$\boldsymbol{E_g}$ (ev)	1.99	1.95	2.1	1.94	2.51
$\boldsymbol{\sigma}$ (s/m)	3	3.08	2.3	3.5	0.3
$\boldsymbol{\varepsilon'}$	5.77	5.76	4.98	6.83	
$\boldsymbol{\varepsilon''}$	6.87	6.88	5.1	7.8	
$\boldsymbol{R}$	49.9%	50%	45%	52%	
$\boldsymbol{Z/Z_0}$	0.333	0.333	0.37	0.31	
$\boldsymbol{\delta_s}$ (mm)	3.1905	3.1902	3.7	3	
$\boldsymbol{SE}$ (db)	1.24	1.24	1	1.4	

Chapter Four

Discussions and Conclusions

In this thesis, the Ag NPs were successfully synthesized using the MW method. Different parameters were controlled during the work, these include the MW power (ML, M, MH, and H), the MW heating time (30s and 90s) and the $AgNO_3$: PVP ratio $(1:1/2, 1:1, 1:2, 1:3)$. A brief study of the optical, electrical and morphological properties was done.

It is concluded from the UV-Vis absorption spectroscopy results of the absorbance values in different wavelengths that all samples have maximum peaks in the expected region for having Ag NPs $(400-450\text{nm})$. This peaks which is denoted by SPR make a red shift towards the higher wavelengths when one of these conditions satisfied: the MW power increase, the MW heating time increase, or the PVP ratio decrease. This red shift is also accompanying with increasing the width of the peak. In addition, the decrease in the PVP ratio has a higher effect than increasing the MW power or heating time. The red shift and smaller energy gaps can be obtained by increasing the MW power or decreasing the PVP ratio.

It is clear from the AFM analysis that the Ag NPs can be formed in the both used MW heating time. All samples have the same nanoparticles shape which is spherical, but with different sizes which affected by the controlled parameters. From the obtained AFM figures, the samples with larger width and larger red shift in the absorbance spectrum plot corresponding to larger Ag NPs sizes. The larger sizes of NPs obtained by increasing the MW power, MW heating time, or decreasing the PVP ratio.

Moreover, studying the electrical properties of the prepared samples by the VNA shows that the 30s samples are not stable. This understood from the unexpected behavior of the electrical conductivity values, also these results change over time. So, the 30s samples cannot been used successfully in applications. By representing the electrical properties of the 90s samples, it is clear that these samples are stable. The electrical conductivity of the 90s samples is much higher than that for the 30s samples (comparing samples with constant MW power and $AgNO_3$: PVP ratio). The measurements of the 90s samples repeated different times during 7 months and gives

approximately the same results in each time. Because of that, the 90s samples can be used in several applications.

From the 11 prepared Ag NPs samples, sample number 9 (MH power for 90s MW heating time and $1:1/2$ ratio) has the highest value of electrical conductivity over all samples. This satisfied at all frequency range ($2-14$ GHz). As a result, this sample also has the largest reflection coefficient which means it can be used as a good shielding material in the EM shielding applications.

These results indicate that the increase of MW power and decrease in the PVP ratio would have an adverse effect on the impedance matching performance of the absorber which was more obvious in the high frequency range with higher electromagnetic energy. In addition, these conditions make an enhancement of the electrical properties of the formed Ag NPs

Future work: adding the best sample for shielding (sample 9) to Multi wall carbon nanotubes (MWCNTs). This new composite may improve the dielectric properties of the MWCNTs. The concentration of the added Ag NPs could be controlled to find the best ratio.

List of Abbreviations

Abbreviations	Meaning
NPs	Nanoparticles
nm	Nanometer
Ag	Silver
MW	Microwave-assisted synthesis method
$tan\delta$	Electric loss tangent
ε_r	Complex permittivity
$\acute{\varepsilon}$	Real part of complex permittivity
$\acute{\acute{\varepsilon}}$	Imaginary part of complex permittivity
σ	Electrical conductivity
Z	Impedance of the material
$Z0$	Impedance of air
$Z/Z0$	Impedance matching ratio
δ_s	Penetration depth (skin depth)
e	Euler's number
α	Attenuation constant
R	Reflection coefficient
SE	Shielding effectiveness
S-Parameters	Scattering parameters
A	Absorbance
λ_{max}	Wavelength of maximum absorption
E_c	Energy of the conduction band
h	Planck's constant
c	Speed of light
SPR	Surface-Plasmon resonance
$AgNO_3$	Silver Nitrate
PVP	Polyvinylpyrrolid
VNA	Vector network analyzer
UV-Vis	Ultraviolet-Visible absorption spectroscopy
AFM	Atomic force microscopy
SPM	Scanning probe microscopy

μ_0	Permeability of free space
ε_0	Permittivity of free space
μ_r	Complex permeability
$\acute{\mu}$	Real part of complex permeability
$\acute{\acute{\mu}}$	Imaginary part of complex permeability
f	Frequency
GHz	Giga Hertz
EM	Electromagnetic wave
w	Angular frequency
E_g	Energy band gap
a	Absorption coefficient
v	Frequency of photon
ev	Electron volt
s/m	Siemens per meter
db/m	Decibel per meter
MWCNTs	Multi wall carbon nanotubes

References

(1) Mohajerani A, Burnett L, Smith JV, Kurmus H, Milas J, Arulrajah A, et al. Nanoparticles in Construction Materials and Other Applications, and Implications of Nanoparticle Use. Materials. 2019 Jan;12(19):3052.

(2) Liu WT. Nanoparticles and their biological and environmental applications. J Biosci Bioeng. 2006 Jul 1;102(1):1–7.

(3) Edmundson MC, Capeness M, Horsfall L. Exploring the potential of metallic nanoparticles within synthetic biology. New Biotechnol. 2014 Dec 25;31(6):572–8.

(4) Pal A, Shah S, Devi S. Microwave-assisted synthesis of silver nanoparticles using ethanol as a reducing agent. Mater Chem Phys. 2009 Apr 15;114(2):530–2.

(5) Pryshchepa O, Pomastowski P, Buszewski B. Silver nanoparticles: Synthesis, investigation techniques, and properties. Adv Colloid Interface Sci. 2020 Oct 1;284:102246.

(6) Morsali A, Hashemi L. Chapter Two - REMOVED: Nanoscale coordination polymers: Preparation, function and application. In: Ruiz-Molina D, van Eldik R, editors. Advances in Inorganic Chemistry [Internet]. Academic Press; 2020 [cited 2024 Sep 22]. p. e1. (Nanoscale Coordination Chemistry; vol. 76). Available from: https://www.sciencedirect.com/science/article/pii/S0898883820300210

(7) Bouafia A, Laouini SE, Ahmed ASA, Soldatov AV, Algarni H, Feng Chong K, et al. The Recent Progress on Silver Nanoparticles: Synthesis and Electronic Applications. Nanomaterials. 2021 Sep;11(9):2318.

(8) Abbas R, Luo J, Qi X, Naz A, Khan IA, Liu H, et al. Silver Nanoparticles: Synthesis, Structure, Properties and Applications. Nanomaterials. 2024 Jan;14(17):1425.

(9) Amsh. Surface area to volume ratio in nanoparticles | Winner Science [Internet]. 2012 [cited 2024 Dec 23]. Available from: https://winnerscience.com/surface-area-to-volume-ratio-in-nanoparticles/

(10) Taylor-Smith K. AZoQuantum. 2020 [cited 2024 Dec 23]. An Introduction to the Quantum Mechanics of Nanoparticles. Available from: https://www.azoquantum.com/Article.aspx?ArticleID=179

(11) Rosso DM. Synthesis and characterization of gold nanoparticles.

(12) Yamamoto T, Wada Y, Sakata T, Mori H, Goto M, Hibino S, et al. Microwave-assisted Preparation of Silver Nanoparticles. Chem Lett. 2004 Feb 1;33(2):158–9.

(13) Britannica, T. E of E. Silver | Facts, Properties, & Uses | Britannica [Internet]. [cited 2024 Sep 22]. Available from: https://www.britannica.com/science/silver

(14) Joshi L. Green Synthesis/Biosynthesis of Silver Nanoparticles by Using Orange Peel Extract. 2018;

(15) Pryshchepa O, Pomastowski P, Buszewski B. Silver nanoparticles: Synthesis, investigation techniques, and properties. Adv Colloid Interface Sci. 2020 Oct;284:102246.

(16) Jamkhande PG, Ghule NW, Bamer AH, Kalaskar MG. Metal nanoparticles synthesis: An overview on methods of preparation, advantages and disadvantages, and applications. J Drug Deliv Sci Technol. 2019 Oct;53:101174.

(17) Dahiya MS, Tomer VK, Duhan S. 31 - Metal–ferrite nanocomposites for targeted drug delivery. In: Inamuddin, Asiri AM, Mohammad A, editors. Applications of Nanocomposite Materials in Drug Delivery [Internet]. Woodhead Publishing; 2018 [cited 2024 Sep 22]. p. 737–60. (Woodhead Publishing Series in Biomaterials). Available from: https://www.sciencedirect.com/science/article/pii/B9780128137413000327

(18) Saleh T, Majeed S, Nayak A, Bhushan B. Principles and Advantages of Microwave-Assisted Methods for the Synthesis of Nanomaterials for Water Purification. In: Advanced Nanomaterials for Water Engineering, Treatment, and Hydraulics. 2017.

(19) Kumar A, Kuang Y, Liang Z, Sun X. Microwave chemistry, recent advancements, and eco-friendly microwave-assisted synthesis of nanoarchitectures and their applications: a review. Mater Today Nano. 2020 Aug 1;11:100076.

(20) Permittivity | Dielectric, Electric Field & Capacitance | Britannica [Internet]. 2024 [cited 2025 Jan 6]. Available from: https://www.britannica.com/science/permittivity

(21) ABS-CS-RF Microwave Absorbers-Laird_081214.pdf [Internet]. [cited 2024 Sep 22]. Available from: https://www.laird.com/sites/default/files/2018-11/ABS-CS-RF%20Microwave%20Absorbers-Laird_081214.pdf

(22) Wei B, Zhou J, Yao Z, Haidry AA, Guo X, Lin H, et al. The effect of Ag nanoparticles content on dielectric and microwave absorption properties of β-SiC. Ceram Int. 2020 Apr 1;46(5):5788–98.

(23) Loss Tangent - an overview | ScienceDirect Topics [Internet]. [cited 2025 Jan 6]. Available from: https://www.sciencedirect.com/topics/physics-and-astronomy/loss-tangent

(24) Asha AB, Narain R. Nanomaterials properties. In: Polymer Science and Nanotechnology [Internet]. Elsevier; 2020 [cited 2025 Jan 6]. p. 343–59. Available from: https://linkinghub.elsevier.com/retrieve/pii/B9780128168066000157

(25) Understanding Impedance Matching - Technical Articles [Internet]. [cited 2024 Sep 22]. Available from: https://eepower.com/technical-articles/understanding-impedance-matching/

(26) Feng Y, Li T, Ge K, Wang X, Wen G, Ye J, et al. Impedance matching strategy boost excellent wave absorption performance of zinc-Aluminosilicate cladded short carbon fiber core-sheath structure. Mater Res Bull. 2022 Sep 1;153:111872.

(27) Liu J, Saw RE, Kiang YH. Calculation of Effective Penetration Depth in X-Ray Diffraction for Pharmaceutical Solids. J Pharm Sci. 2010 Sep 1;99(9):3807–14.

(28) Microwave Technology | Penetration Depths [Internet]. [cited 2025 Jan 6]. Available from: https://www.pueschner.com/en/microwave-technology/penetration-depths

(29) Nondestructive Evaluation Physics : Waves [Internet]. [cited 2025 Jan 6]. Available from: https://www.nde-ed.org/Physics/Waves/reflectiontransmission.xhtml

(30) Electromagnetic shielding theory | Electromagnetic Interference Class Notes | Fiveable [Internet]. [cited 2024 Sep 22]. Available from: https://library.fiveable.me/electromagnetic-interference-and-compatibility/unit-4/electromagnetic-shielding-theory/study-guide/NtdVDH4ZNu9VDShl

(31) Gooch JW, Daher JK. Fundamentals of Electromagnetic Shielding. In: Gooch JW, Daher JK, editors. Electromagnetic Shielding and Corrosion Protection for Aerospace Vehicles [Internet]. New York, NY: Springer; 2007 [cited 2025 Jan 6]. p. 17–24. Available from: https://doi.org/10.1007/978-0-387-46096-3_3

(32) S-Parameters Basics | EMA Design Automation [Internet]. 2023 [cited 2024 Nov 26]. Available from: https://www.ema-eda.com/ema-resources/blog/s-parameters-basics/

(33) ThoughtCo [Internet]. [cited 2024 Sep 22]. What Does Absorbance Mean in Chemistry? Available from: https://www.thoughtco.com/definition-of-absorbance-604351

(34) Gharibshahi L, Saion E, Gharibshahi E, Shaari AH, Matori KA. Structural and Optical Properties of Ag Nanoparticles Synthesized by Thermal Treatment Method. Materials. 2017 Apr;10(4):402.

(35) Jana J, Ganguly M, Pal T. Enlightening surface plasmon resonance effect of metal nanoparticles for practical spectroscopic application. RSC Adv. 2016 Sep 8;6(89):86174–211.

(36) nanoComposix [Internet]. [cited 2024 Nov 28]. Silver Nanoparticles: Optical Properties. Available from: https://nanocomposix.com/pages/silver-nanoparticles-optical-properties

(37) Hamad OA. SYNTHESIS, ANALYTICAL AND SPECTROSCOPIC CHARACTERIZATION OF NOVEL NANOPARTICLES /NANOPIGMENTS USING A MICROWAVE ASSISTED METHOD.

(38) Chook SW, Chia CH, Zakaria S, Ayob MK, Chee KL, Huang NM, et al. Antibacterial performance of Ag nanoparticles and AgGO nanocomposites prepared via rapid microwave-assisted synthesis method. Nanoscale Res Lett. 2012 Sep 28;7(1):541.

(39) Hong X, Wen J, Xiong X, Hu Y. Shape effect on the antibacterial activity of silver nanoparticles synthesized via a microwave-assisted method. Environ Sci Pollut Res. 2016 Mar 1;23(5):4489–97.

(40) Tang C, Xing B, Hu G, Huang F, Zuo C. A facile microwave approach to the fast-and-direct production of silver nano-ink. Mater Lett. 2017 Feb 1;188:220–3.

(41) Beyene HD, Werkneh AA, Bezabh HK, Ambaye TG. Synthesis paradigm and applications of silver nanoparticles (AgNPs), a review. Sustain Mater Technol. 2017 Sep 1;13:18–23.

(42) Microwave-Assisted Synthesis of Silver Nanoparticles: Effect of Reaction Temperature and Precursor Concentration on Fluorescent Property | Journal of Cluster Science [Internet]. [cited 2024 Sep 23]. Available from: https://link.springer.com/article/10.1007/s10876-020-01945-x

(43) Manno R, Sebastian V, Irusta S, Mallada R, Santamaria J. Ultra-Small Silver Nanoparticles Immobilized in Mesoporous SBA-15. Microwave-Assisted Synthesis and Catalytic Activity in the 4-Nitrophenol Reduction. Catal Today. 2021 Feb 15;362:81–9.

(44) Sreeram KJ, Nidhin M, Nair BU. Microwave assisted template synthesis of silver nanoparticles. Bull Mater Sci. 2008 Dec 1;31(7):937–42.

(45) Gupta S, Giordano C, Gradzielski M, Mehta SK. Microwave-assisted synthesis of small Ru nanoparticles and their role in degradation of congo red. J Colloid Interface Sci. 2013 Dec;411:173–81.

(46) Sutradhar P, Debnath N, Saha M. Microwave-assisted rapid synthesis of alumina nanoparticles using tea, coffee and triphala extracts. Adv Manuf. 2013 Dec;1(4):357–61.

(47) Vijayakumar S, Ponnalagi AK, Nagamuthu S, Muralidharan G. Microwave assisted synthesis of Co3O4 nanoparticles for high-performance supercapacitors. Electrochimica Acta. 2013 Sep;106:500–5.

(48) Kajbafvala A, Ghorbani H, Paravar A, Samberg JP, Kajbafvala E, Sadrnezhaad SK. Effects of morphology on photocatalytic performance of Zinc oxide nanostructures synthesized by rapid microwave irradiation methods. Superlattices Microstruct. 2012 Apr;51(4):512–22.

(49) Pratheepa MI, Lawrence M. Synthesis of pure, Cu and Zn doped CdO nanoparticles by co-precipitation method for supercapacitor applications. Vacuum. 2019 Apr;162:208–13.

(50) Zhang XF, Liu ZG, Shen W, Gurunathan S. Silver Nanoparticles: Synthesis, Characterization, Properties, Applications, and Therapeutic Approaches. Int J Mol Sci. 2016 Sep 13;17(9):1534.

(51) Xu L, Wang YY, Huang J, Chen CY, Wang ZX, Xie H. Silver nanoparticles: Synthesis, medical applications and biosafety. Theranostics. 2020 Jul 11;10(20):8996–9031.

(52) Abou El-Nour KMM, Eftaiha A, Al-Warthan A, Ammar RAA. Synthesis and applications of silver nanoparticles. Arab J Chem. 2010 Jul;3(3):135–40.

(53) Jasni AH, Ali AA, Sagadevan S, Wahid Z, Jasni AH, Ali AA, et al. Silver Nanoparticles in Various New Applications. In: Silver Micro-Nanoparticles - Properties, Synthesis, Characterization, and Applications [Internet]. IntechOpen; 2021 [cited 2025 Jan 7]. Available from: https://www.intechopen.com/chapters/75294

(54) Lee SH, Jun BH. Silver Nanoparticles: Synthesis and Application for Nanomedicine. Int J Mol Sci. 2019 Feb 17;20(4):865.

(55) Chemistry LibreTexts [Internet]. 2017 [cited 2024 Sep 29]. 1.4K: Reflux. Available from: https://chem.libretexts.org/Bookshelves/Organic_Chemistry/Organic_Chemistry_Lab_Techniques_(Nichols)/01%3A_General_Techniques/1.04%3A_Heating_and_Cooling_Methods/1.4K%3A_Reflux

(56) What Are Vector Network Analyzers? | VNAs Explained [Internet]. [cited 2025 Jan 7]. Available from: https://www.tek.com/en/documents/primer/what-vector-network-analyzer-and-how-does-it-work

(57) DIELECTRIC SPECTROSCOPY: AN OVERVIEW » SPEAG, Schmid & Partner Engineering AG [Internet]. [cited 2024 Sep 30]. Available from: https://speag.swiss/products/dak/dielectric-spectroscopy-an-overview/

(58) AN_DAK_DAKS Best Practices.pdf [Internet]. [cited 2024 Sep 30]. Available from:

https://speag.swiss/assets/downloads/products/dak/free_downloads/AN_DAK_DAKS%20Best%20Practices.pdf

(59) Tissue BM. Ultraviolet and Visible Absorption Spectroscopy. In: Characterization of Materials [Internet]. John Wiley & Sons, Ltd; 2002 [cited 2024 Oct 4]. Available from: https://onlinelibrary.wiley.com/doi/abs/10.1002/0471266965.com059

(60) Principle, Instrument Design, Methods and Applications of UV: A Comprehensive Guide [Internet]. Unacademy. [cited 2024 Oct 4]. Available from: https://unacademy.com/content/kerala-psc/study-material/bioinstrumentation/principle-instrument-design-methods-and-applications-of-uv-a-comprehensive-guide/

(61) JoVE [Internet]. [cited 2024 Dec 24]. Ultraviolet-Visible (UV-Vis) Spectroscopy. Available from: https://www.jove.com/v/10204/ultraviolet-visible-uv-vis-spectroscopy-principle-and-uses

(62) band-gap-analysis-uv-visible-spectroscopy-an54685-en.pdf [Internet]. [cited 2024 Nov 28]. Available from: https://assets.thermofisher.com/TFS-Assets/CAD/Application-Notes/band-gap-analysis-uv-visible-spectroscopy-an54685-en.pdf

(63) Park Systems [Internet]. [cited 2024 Oct 5]. Available from: https://www.parksystems.com/en/learning-center/html

(64) AFM – Atomic Force Microscopy | Science SAVED - Scientific Analysis Vitalises Enterprise Development [Internet]. [cited 2025 Jan 7]. Available from: https://science-saved.com/en/afm

(65) Gwyddion – Free SPM (AFM, SNOM/NSOM, STM, MFM, …) data analysis software [Internet]. [cited 2024 Dec 24]. Available from: https://gwyddion.net/

(66) Al-Gaashani R, Radiman S, Tabet N, Daud AR. Effect of microwave power on the morphology and optical property of zinc oxide nano-structures prepared via a microwave-assisted aqueous solution method. Mater Chem Phys. 2011 Feb;125(3):846–52.

(67) He B, Tan JJ, Liew KY, Liu H. Synthesis of size controlled Ag nanoparticles. J Mol Catal Chem. 2004 Nov;221(1–2):121–6.

(68) Lalitha Devi B, Mohan Rao K, Ramananda D. Effect of microwave irradiation time on structural and optical properties of ZnS nanoparticles. Inorg Chem Commun. 2022 Jun 1;140:109460.

(69) Vuppalapati L, Masilamani K, Velayutham R, Venkateshan N, D.V.R. S, CK AK, et al. Promising upshot of silver nanoparticles primed from Gracilaria crassa against bacterial pathogens. Chem Cent J. 2015 Aug 7;9:42.

(70) Amirjani A, Firouzi F, Haghshenas DF. Predicting the Size of Silver Nanoparticles from Their Optical Properties. Plasmonics. 2020 Aug;15(4):1077–82.

(71) Saadoun H, Jabbar AT, Kamil AS. Investigation of energy band gap and the synthesis of silver nanoparticles. AIP Conf Proc. 2024 Mar 15;3036(1):050021.

(72) Aziz A, Khalid M, Akhtar MS, Nadeem M, Gilani ZA, Ullah Z, et al. STRUCTURAL, MORPHOLOGICAL AND OPTICAL INVESTIGATIONS OF SILVER NANOPARTICLES SYNTHESIZED BY SOL-GEL AUTO-COMBUSTION METHOD.

(73) Yuliza E, Murniati R, Rajak A, Khairurrijal K, Abdullah M. Effect of Particle Size on the Electrical Conductivity of Metallic Particles. 2014.

(74) Liu P, Yao Z, Zhou J, Yang Z, Kong LB. Small magnetic Co-doped NiZn ferrite/graphene nanocomposites and their dual-region microwave absorption performance. J Mater Chem C. 2016 Oct 20;4(41):9738–49.

(75) What is Yield?-Definition, Types, and Examples – Master Chemistry [Internet]. 2023 [cited 2025 Jan 7]. Available from: https://themasterchemistry.com/what-is-yield-in-chemistry/

Appendices

Appendix A

Figures of Study

Figure.1

Schematic diagram of SPR process

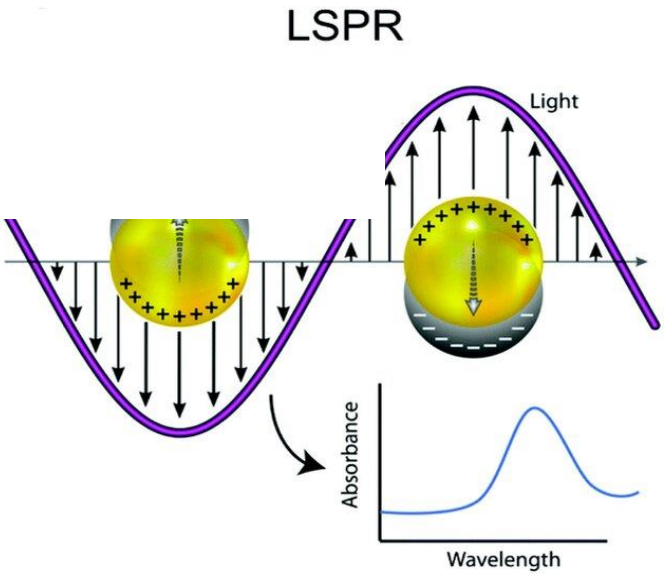

Figure.2

Schematic diagram of Energy band gap for bulk and nanomaterials

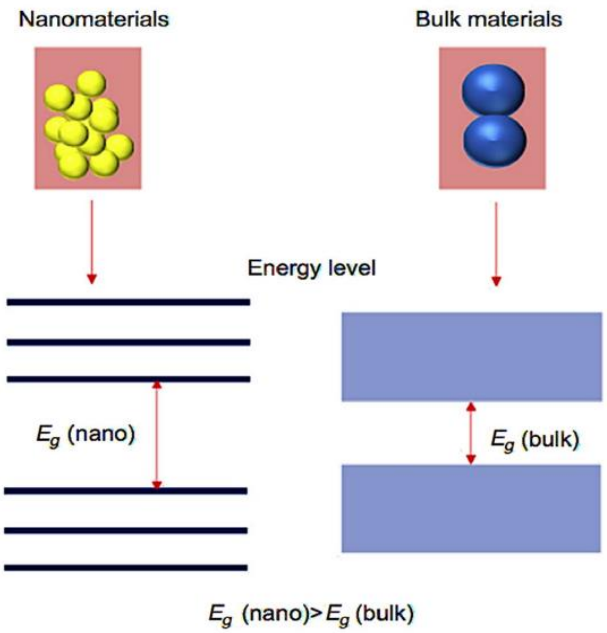

Figure.3

Schematic diagram of microwave heating process

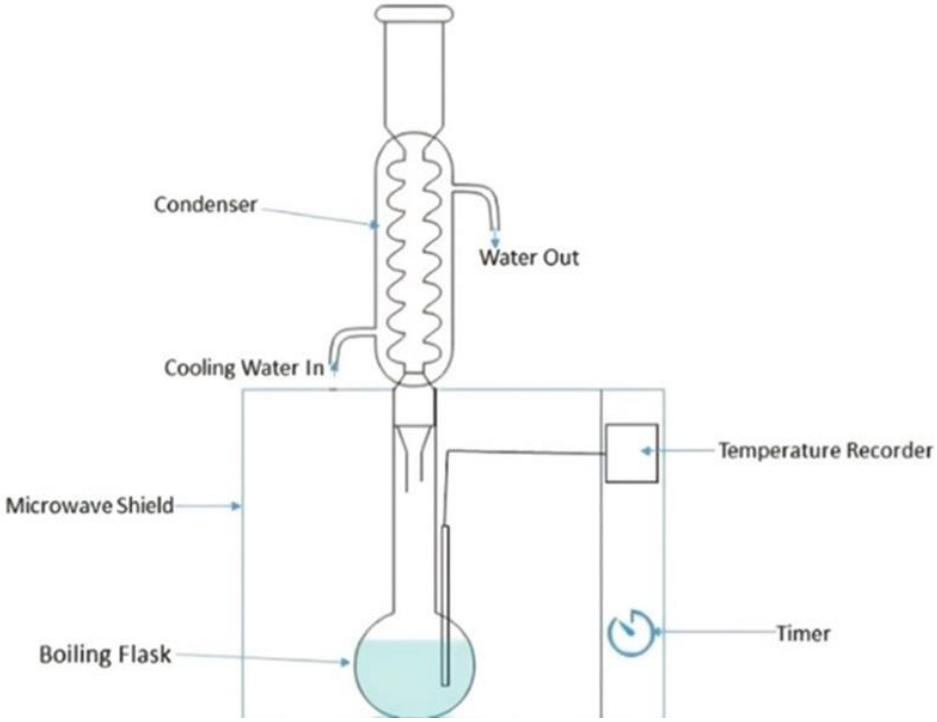

Figure.4

Schematic diagram of the working principle of the UV-Vis absorption spectroscopy

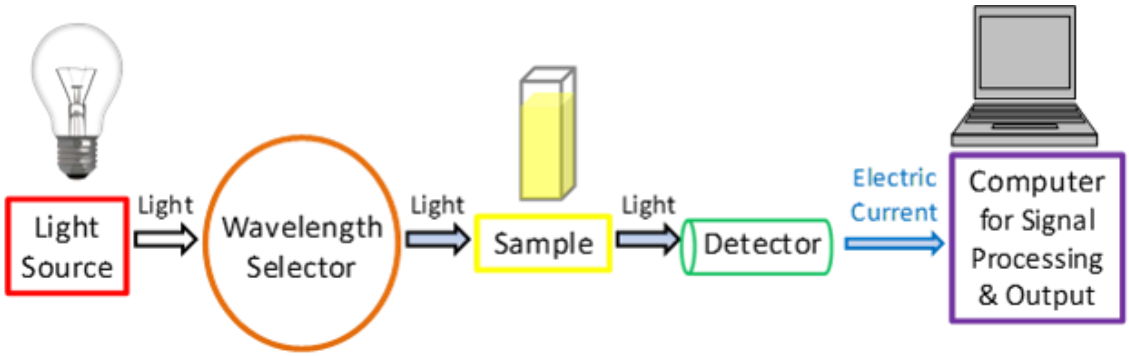

Figure.5

Electrical conductivity of 30s Ag NPs samples with different MW powers

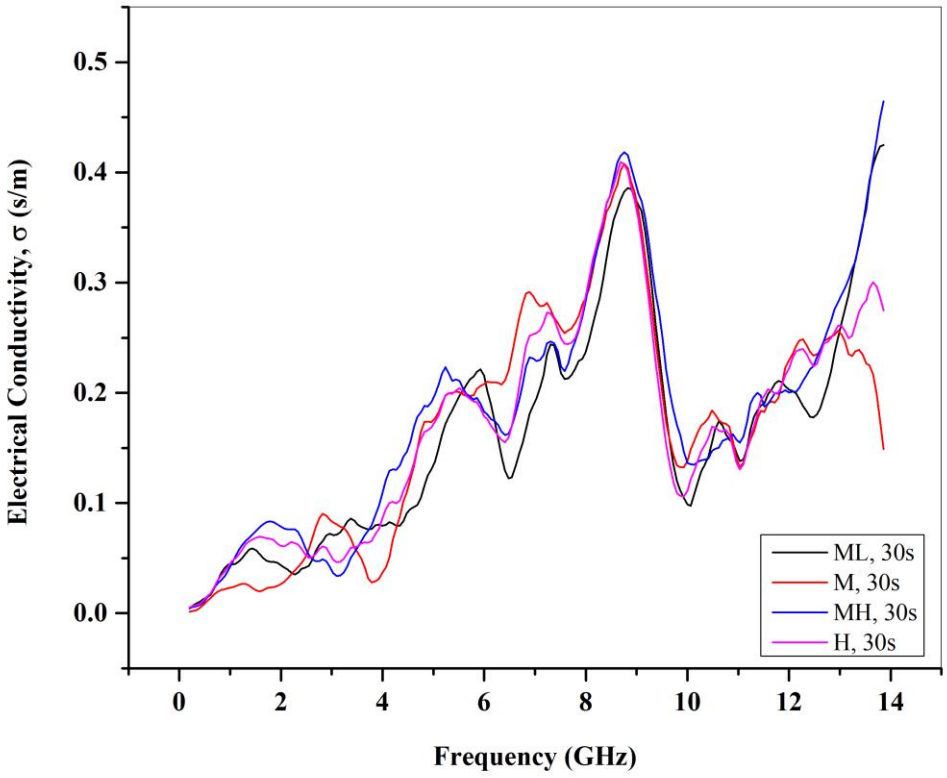

Figure.6

*The Reflection coefficient as a function of frequency. (a) Shows **R** for different MW powers. (b) Shows **R** for different $AgNO_3$: PVP ratios*

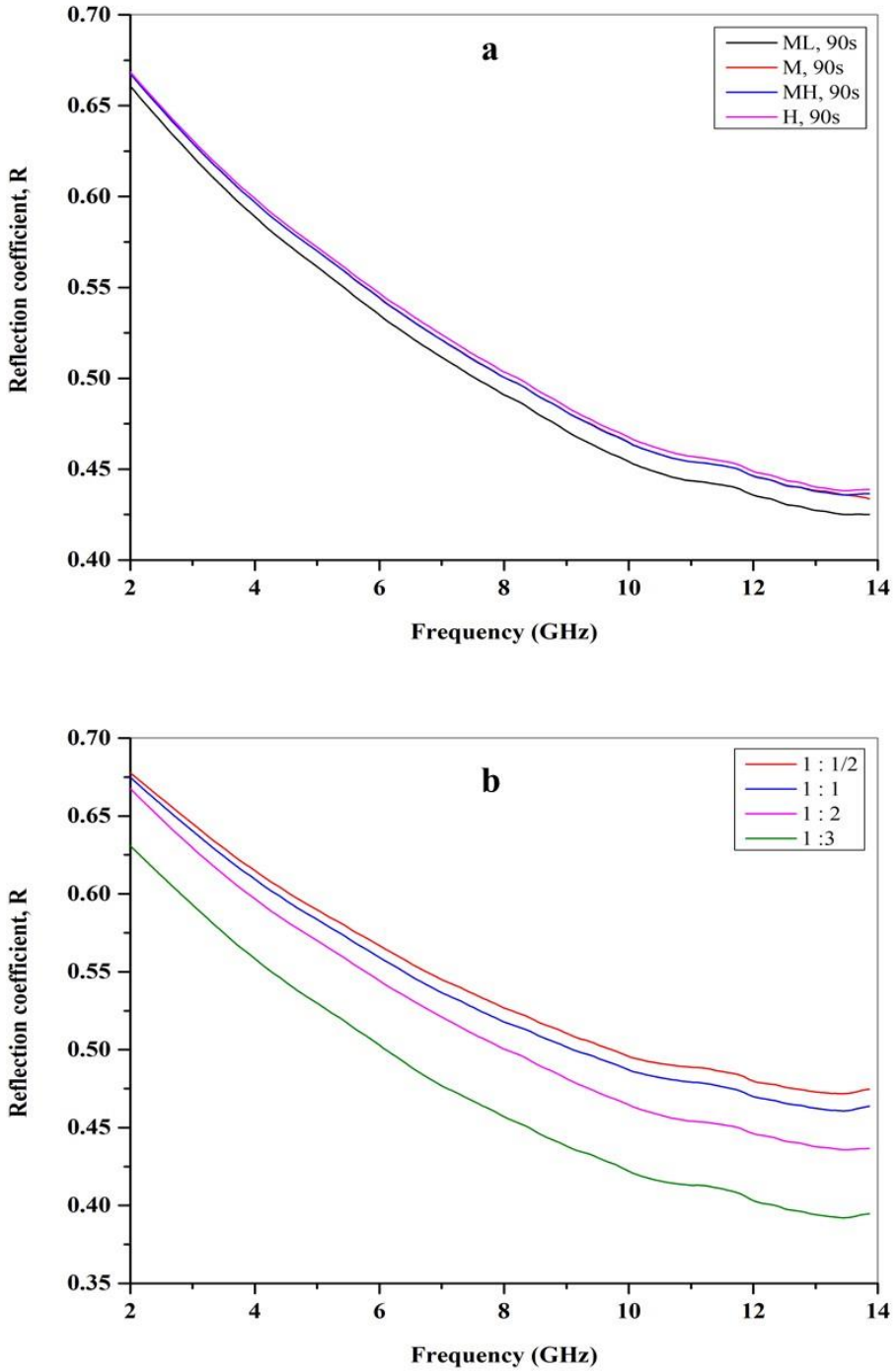

Figure.7

The Shielding effectiveness as a function of frequency. (a) Shows ***SE*** *for different MW powers. (b) Shows* ***SE*** *for different $AgNO_3$: PVP ratios*

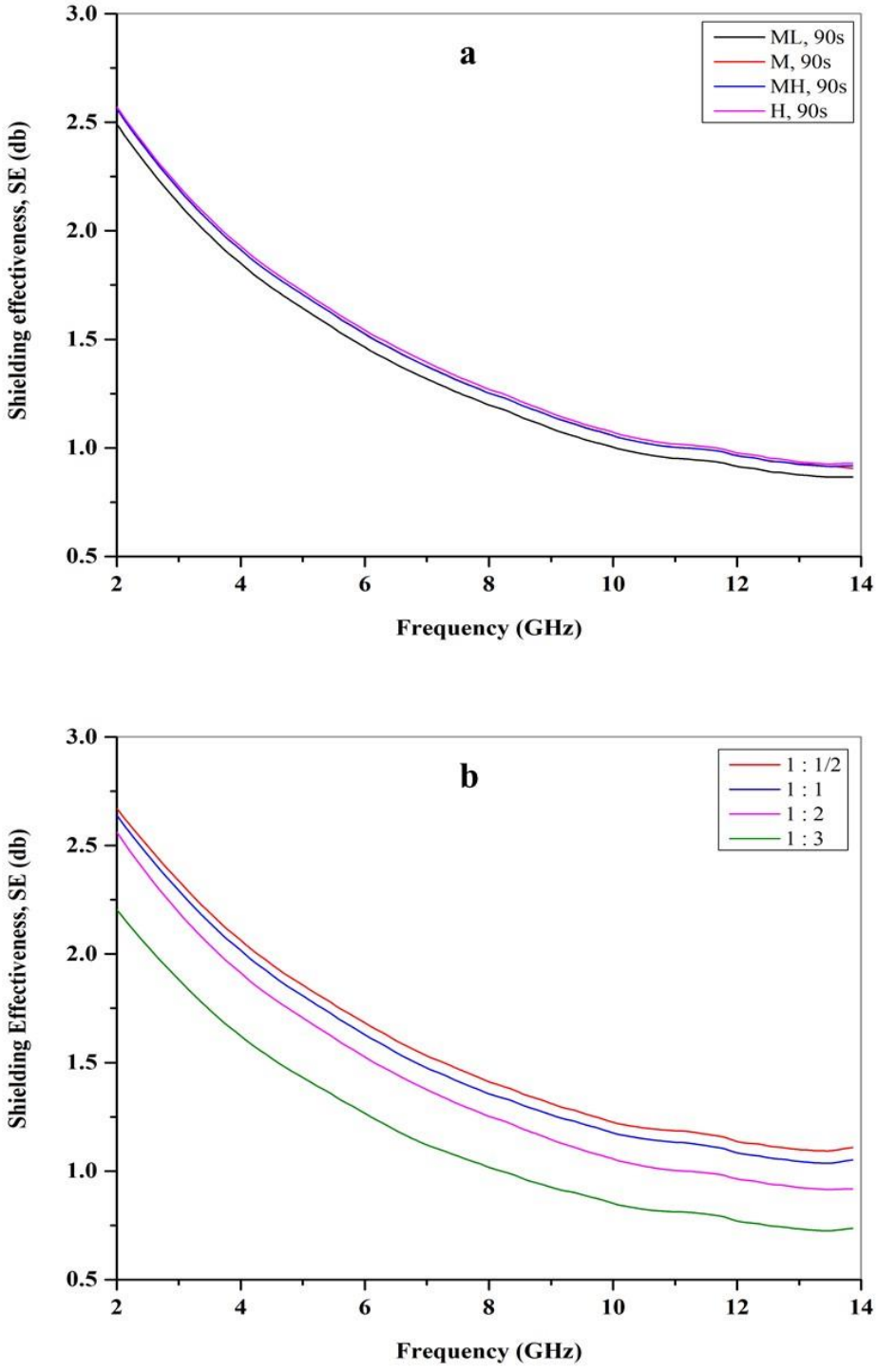

Figure.8

Evaporation process of the Ag NPs to get the yield

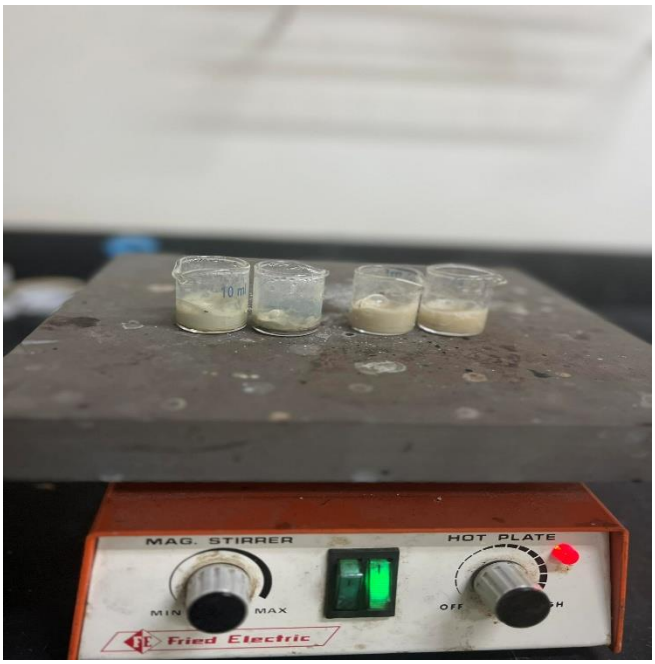

Figure.9

Electrical conductivity of 60s Ag NPs samples with different MW powers, data were taken in two different days

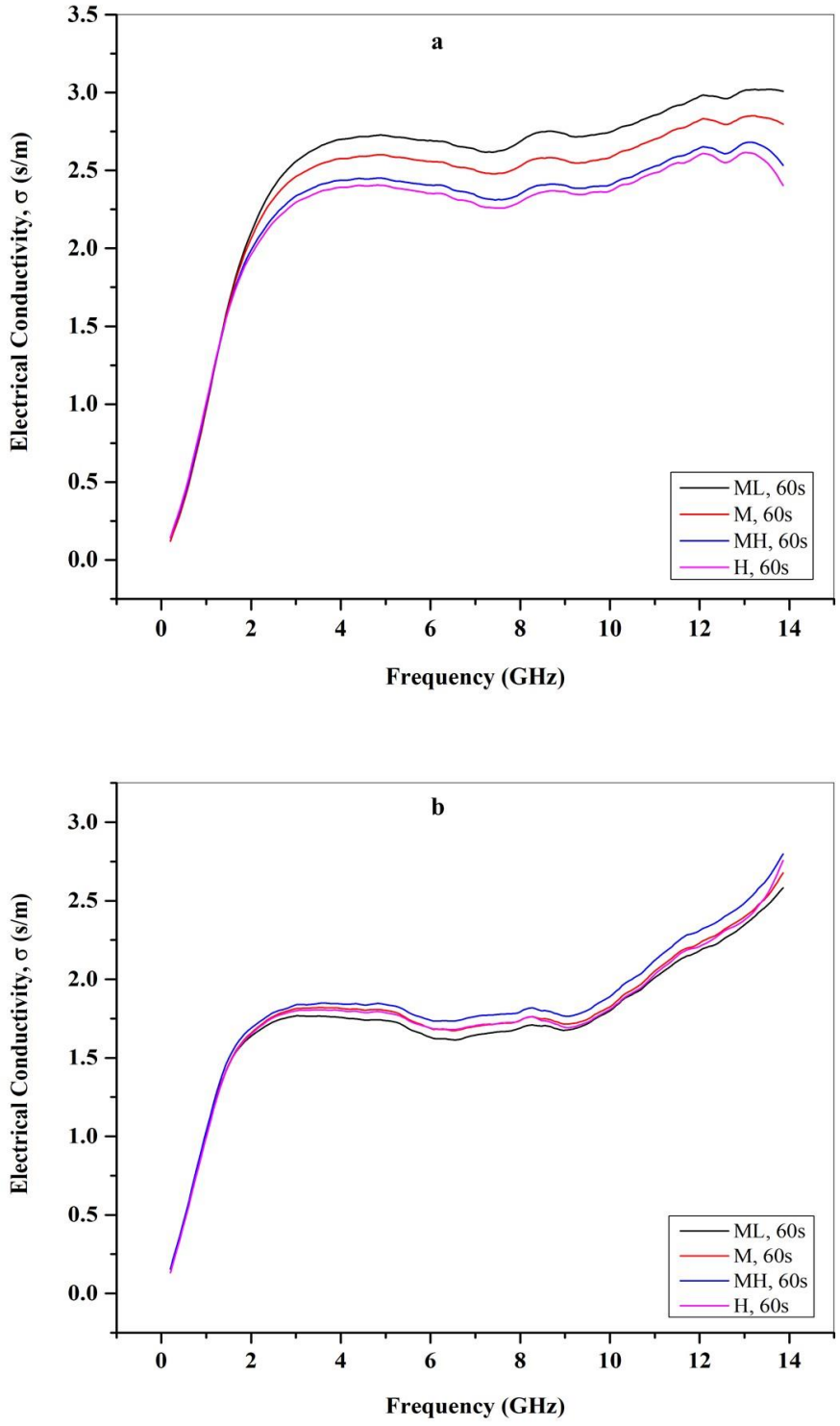

جـامعـــة النجاح الوطنية

كليـــة الدراســـات العليـــا

دراسة الخصائص الكهربائية والبصرية والمورفولوجية لجسيمات الفضة النانوية المحضرة بطريقة الميكروويف

إعداد

شهد سعد الله فايق هباش

إشراف

د. منى حاج يحيى

د. معن اشتيوي

قدمت هذه الرسالة استكمالاً لمتطلبات الحصول على درجة الماجستير في الفيزياء، من كلية الدراسات العليا، في جامعة النجاح الوطنية، نابلس– فلسطين

2025

دراسة الخصائص الكهربائية والبصرية والمورفولوجية لجسيمات الفضة النانوية المحضرة بطريقة الميكروويف

إعداد

شهد سعد الله فايق هباش

إشراف

د. منى حاج يحيى

د. معن اشتيوي

الملخص

الجسيمات النانوية هي جسيمات صغيرة جداً، يتراوح قطرها ما بين 1–100 نانوميتر. تدخل الجسيمات النانوية الفلزية في كثير من الأبحاث الحديثة، وذلك لأهميتها في مختلف المجالات (الكهربائية والبصرية والصناعية وغيرها). يعتبر عنصر الفضة من أكثر الفلزات تميزاً وذلك نظراً لخصائصها الفيزيائية والكيميائية المميزة.

تم استخدام طرق عديدة في تحضير جسيمات الفضة النانوية، و تعتبر طريقة التحضير باستخدام الميكروويف من أفضل الطرق المستخدمة، إذ يتم من خلالها تصنيع الجسيمات في وقت قصير نسبياً (لا يتجاوز البضع دقائق أو ثواني)، وأيضاً يتم الحصول على كمية وفيرة من الجسيمات النانوية، كما يمكن التحكم بطريقة التحضير من خلال عدة متغيرات والذي ينعكس على طبيعة الجسيمات النانوية المتكونة.

في هذه الدراسة قمنا بتحضير جسيمات الفضة النانوية باستخدام طريقة الميكروويف. تم استخدام نترات الفضة كمصدر لجسيمات الفضة، بإضافة الإيثيلين جلايكول كعامل اختزال والبولي فينيل بيروليد كعامل تثبيت. تمت هذه الدراسة بالتحكم بعدة متغيرات خلال عملية التحضير وهي: طاقة الميكروويف (متوسط_منخفض، متوسط، متوسط_عالي، عالي)، وزمن التسخين بالميكروويف (30 ثانية و90 ثانية)، كما تم التحكم أيضاً بنسبة نترات الفضة المستخدمة إلى عامل التثبيت.

تمت دراسة الخصائص البصرية والمورفولوجية والكهربائية لجسيمات الفضة النانوية المتكونة من خلال محلل الطيف للأشعة المرئية وفوق البنفسجية، ومجهر القوة الذرية ومحلل شبكة المتجهات.

تبيّن مما سبق أن الزمنين كافيين لتحضير جسيمات الفضة النانوية، وذلك من خلال قيمة الطول الموجي لأعلى امتصاص والذي وقع ضمن المنطقة الصحيحة لتكوّن هذه الجسيمات. وباستخدام مجهر القوة الذرية كان شكل الجسيمات في جميع الحالات كروياً بأحجام مختلفة. إلّا أن العينات التي تم تحضيرها على زمن 30 ثانية لم تحقق الثبات بخصائصها الكهربائية، على عكس العينات التي تعرضت للتسخين لمدة 90 ثانية والتي حققت ثبات عالي في جميع خصائصها.

الكلمات المفتاحية: جسيمات الفضة النانوية، طريقة التحضير بالميكروويف، مجهر القوة الذرية، محلل الطيف للأشعة المرئية وفوق البنفسجية، محلل شبكة المتجهات.